

Manuscript version: Author's Accepted Manuscript

The version presented in WRAP is the author's accepted manuscript and may differ from the published version or Version of Record.

Persistent WRAP URL:

<http://wrap.warwick.ac.uk/136531>

How to cite:

Please refer to published version for the most recent bibliographic citation information. If a published version is known of, the repository item page linked to above, will contain details on accessing it.

Copyright and reuse:

The Warwick Research Archive Portal (WRAP) makes this work by researchers of the University of Warwick available open access under the following conditions.

© 2020 Elsevier. Licensed under the Creative Commons Attribution-NonCommercial-NoDerivatives 4.0 International <http://creativecommons.org/licenses/by-nc-nd/4.0/>.



Publisher's statement:

Please refer to the repository item page, publisher's statement section, for further information.

For more information, please contact the WRAP Team at: wrap@warwick.ac.uk.

Lateral instability of steel beams in fire: Behaviour, numerical modelling and design

Merih Kucukler

School of Engineering, University of Warwick, Coventry, CV4 7AL, UK

Abstract

The lateral torsional buckling behaviour and design of steel beams in fire are investigated in this paper. Finite element models able to replicate the lateral-torsional buckling (LTB) response of steel beams at elevated temperatures are developed and validated. The validated finite element models are used to carry out extensive parametric studies to explore the LTB behaviour of steel beams in fire, considering various cross-section shapes, member slendernesses, steel grades, elevated temperature levels and different fabrication processes. A design equation for the LTB assessment of steel beams at elevated temperatures is developed on the basis of the results from the extensive parametric studies. The high accuracy, safety and reliability of the proposed design approach are illustrated, which is also compared against the beam design rules existing in the European structural steel fire design standard EN 1993-1-2. The design proposals made in this paper are compatible with the new LTB assessment equations that are due to be incorporated into the next version of the European room temperature structural steel design standard EN 1993-1-1 and lead to more accurate ultimate strength predictions relative to the beam buckling design equations existing in EN 1993-1-2.

Keywords: Finite element modelling, Geometrical imperfections, Fire, Lateral-torsional buckling, Structural steel design method, Residual stresses, Steel beams

1. Introduction

In fire, structural steel beams lose their room temperature strength and stiffness, resulting in significant reductions in their ultimate load carrying capacities which can further reduce due to lateral-torsional buckling (LTB) if they are laterally unrestrained. To ensure the ability of a laterally unrestrained steel beam to continue to withstand forces acting on it in fire, its LTB response at elevated temperatures has to be taken into consideration in its fire design. The European structural steel fire design standard EN 1993-1-2 [1] provides a series of design equations to account for LTB in the design of steel beams at elevated temperatures. However, these design formulae adopt a buckling curve based on the Perry-Robertson equation [2, 3] derived considering the flexural buckling response of columns, thus failing to

Email address: merih.kucukler@warwick.ac.uk (Merih Kucukler)

provide a sound representation of the mechanical response of steel beams experiencing LTB in fire and leading to a rather inconsistent level of accuracy in the prediction of the LTB resistances of steel beams at elevated temperatures.

Recently, new LTB design curves based on a Perry-Robertson equation able to represent the mechanical response of imperfect elastic beams undergoing LTB at room temperature have been derived by Taras and Greiner [4]. It was shown in these studies [4] that once carefully calibrated, this mechanically sound Perry-Robertson equation leads to significantly more accurate ultimate strength predictions relative to the existing beam buckling design rules of the European room temperature structural steel design standard EN 1993-1-1 [5], which use the buckling curves based on the Perry-Robertson equation derived taking into account the flexural buckling response of columns [2, 3]. The LTB design rules proposed by [4] are due to be incorporated into the upcoming version of EN 1993-1-1 [5], which is currently referred to as prEN 1993-1-1 [6].

In spite of these recent advancements in the European room temperature beam buckling assessment rules, there is no study carried out thus far that has focused on the enhancement of the elevated temperature beam buckling design rules in EN 1993-1-2 [1] by using the recently developed Perry-Robertson equation of [4]. The beam buckling design equations set out in EN 1993-1-2 [1] originates from the studies of Vila Real and Franssen [7], where the Perry-Robertson equation originally derived taking into account the flexural buckling response of steel columns at room temperature was recalibrated by considering results from numerical studies on the behaviour of laterally unrestrained steel beams in fire. However, in the development of the beam buckling design equations of EN 1993-1-2 [1], steel beams with only one European cross-section shape (IPE 220) subjected to uniform bending were considered [8]. In view of the consideration of a limited number of cases during their development, Vila Real et al. [8] highlighted room for further improvement of the accuracy of the current EN 1993-1-2 [1] beam buckling assessment rules for different cross-section shapes and loading conditions. Though a number of proposals for the further improvement of the LTB design rules of [1] have been made [8–12], these studies focused on the recalibration of the existing LTB equations of EN 1993-1-2 [1]; a beam design equation able to provide a sound representation of the mechanical response of steel beams experiencing LTB is yet to be calibrated considering the response at elevated temperatures.

With the aim of enhancing the accuracy of the existing beam buckling design rules in EN 1993-1-2 [1] and also satisfying the compatibility between the LTB assessment rules in the European structural steel design codes for room temperature design EN 1993-1-1 [5] and elevated temperature design EN 1993-1-2 [1], which will lack in the upcoming versions of the two design standards due to the introduction of the new beam buckling assessment rules in the former, a research study focusing on the LTB behaviour and design of steel beams in fire is carried out in this paper. Initially, nonlinear shell finite element models of steel beams able to replicate their LTB response at elevated temperatures are developed. The developed finite element models are then validated against experimental results from the literature. Through the Geometrically and Materially Nonlinear Analyses with Imperfections (GMNIA) of the validated finite element models, comprehensive numerical parametric studies are carried out to explore the LTB response of steel beams in fire, considering different elevated temperature

levels, cross-section shapes, steel grades and member slendernesses. On the basis of the large number of results obtained from the extensive numerical parametric studies, the Perry-Robertson equation able to account for the LTB response of imperfect elastic steel beams is calibrated to accurately estimate the LTB strengths of inelastic steel beams in fire. The high accuracy and reliability of the new beam buckling equations relative to the design rules existing in EN 1993-1-2 [1] are illustrated considering a broad range of cases. It should be noted that in this study, the global buckling behaviour and design steel beams in fire are considered; thus, the design method proposed in this paper is applicable to steel beams with Class 1 and 2 cross-sections only. The presented proposals will be extended to beams susceptible combined global and local buckling effects in fire in a future study.

2. Finite element modelling

This section addresses the development of shell finite element models able to replicate the LTB response of steel beams in fire and their validation against experimental results from the literature. The validated finite element models are utilised in the following sections to perform extensive parametric studies to explore factors influencing the LTB response of steel beams in fire and to generate benchmark data for the development of new beam buckling design rules.

2.1. Development of finite element models

The finite element models were created using the finite element analysis software Abaqus [13] in this paper. Designated as S4R in the Abaqus element library, a four-noded, reduced integration shell element able to account for transverse shear deformations and membrane stresses, was utilised to mesh all the finite element models. To accurately consider the elastic-plastic cross-section response and global buckling behaviour, 16 elements were used to model each web and flange plate. The numbers of the elements along the lengths of the members were selected such that the aspect ratios of the elements within the webs were approximately equal to unity. In accordance with the approach adopted by [14–16], the web plates of the beams were offset the half flange thicknesses to avoid the overlapping of the flange and web plates.

To mimic the response of carbon steel beams at elevated temperatures, the four-stage elevated temperature material model given in EN 1993-1-2 [1] for carbon steel shown in Fig. 1 was utilised in accordance with [17–21], defining the elevated temperature stress versus strain relationship through the following expressions:

$$\begin{aligned}
 \sigma &= \epsilon E_{a,\theta} & \text{for } \epsilon \leq \epsilon_{p,\theta}, \\
 \sigma &= f_{p,\theta} - c + (b/a) \sqrt{a^2 - (\epsilon_{y,\theta} - \epsilon)^2} & \text{for } \epsilon_{p,\theta} \leq \epsilon \leq \epsilon_{y,\theta}, \\
 \sigma &= f_{y,\theta} & \text{for } \epsilon_{y,\theta} \leq \epsilon \leq \epsilon_{t,\theta}, \\
 \sigma &= f_{y,\theta} [1 - (\epsilon - \epsilon_{t,\theta}) / (\epsilon_{u,\theta} - \epsilon_{t,\theta})] & \text{for } \epsilon_{t,\theta} \leq \epsilon \leq \epsilon_{u,\theta}
 \end{aligned} \tag{1}$$

where σ and ϵ are the engineering stress and strain and $E_{a,\theta}$, $f_{p,\theta}$ and $f_{y,\theta}$ are the Young's modulus, the proportional limit and the effective yield strength at temperature θ , respectively. In eq. (1), $\epsilon_{p,\theta}$ is the strain at proportional limit calculated as $\epsilon_{p,\theta} = f_{p,\theta} / E_{a,\theta}$, $\epsilon_{y,\theta}$ is

the yield strain equal to 0.02 (i.e. $\epsilon_{y,\theta} = 0.02$), $\epsilon_{t,\theta}$ is the limiting strain for yield strength taken as 0.15 (i.e. $\epsilon_{t,\theta} = 0.15$) and $\epsilon_{u,\theta}$ is the ultimate strain equal to 0.20 (i.e. $\epsilon_{u,\theta} = 0.20$). The auxiliary coefficients a , b and c used in eq. (1) are determined as given below:

$$\begin{aligned} a &= \sqrt{(\epsilon_{y,\theta} - \epsilon_{p,\theta})(\epsilon_{y,\theta} - \epsilon_{p,\theta} + c/E_{a,\theta})}, \\ b &= \sqrt{c(\epsilon_{y,\theta} - \epsilon_{p,\theta})E_{a,\theta} + c^2}, \\ c &= \frac{(f_{y,\theta} - f_{p,\theta})^2}{(\epsilon_{y,\theta} - \epsilon_{p,\theta})E_{a,\theta} - 2(f_{y,\theta} - f_{p,\theta})}. \end{aligned} \quad (2)$$

As shown in Fig. 1 (a), the elevated temperature effective yield strength $f_{y,\theta}$ and proportional limit $f_{p,\theta}$ are calculated by multiplying the elevated temperature yield strength reduction factor $k_{y,\theta}$ and proportional limit reduction factor $k_{p,\theta}$ by the room temperature yield strength f_y (i.e. $f_{y,\theta} = k_{y,\theta}f_y$ and $f_{p,\theta} = k_{p,\theta}f_y$), while the elevated temperature Young's modulus $E_{a,\theta}$ is calculated by multiplying the elevated temperature Young's modulus reduction factor $k_{E,\theta}$ by the room temperature Young's modulus of carbon steel E_a (i.e. $E_{a,\theta} = k_{E,\theta}E_a$). In this paper, the values of $k_{y,\theta}$, $k_{p,\theta}$ and $k_{E,\theta}$ provided in EN 1993-1-2 [1] and illustrated in Fig. 1 (b) were used, where $k_{p0.2,\theta}$ is the elevated temperature 0.2% proof strength reduction factor multiplied by the yield strength f_y to determine the elevated temperature 0.2% proof strength $f_{p0.2,\theta}$ (i.e. $f_{p0.2,\theta} = k_{p0.2,\theta}f_y$). As can be seen from Fig. 1 (b), the Young's modulus reduction $k_{E,\theta}$ is more severe relative to the yield strength reduction $k_{y,\theta}$ for carbon steel in fire, highlighting the increased susceptibility of carbon steel elements to instability at elevated temperatures. In accordance with the approach adopted in [17–20] where Abaqus [13] was also employed to simulate the behaviour of structural steel elements in fire in conjunction with the elevated temperature material model given in EN 1993-1-2 [1], the engineering stress-strain relationship given by eq. (1) was transformed into a true stress-strain relationship for input into finite element models using the following equations:

$$\sigma_{true} = \sigma(1 + \epsilon), \quad (3)$$

$$\epsilon_{true} = \ln(1 + \epsilon), \quad (4)$$

where σ_{true} and ϵ_{true} are the true stress and strain, respectively. It should be noted that EN 1993-1-2 [1] adopts the Rubert and Schaumann [22] material model which was derived on the basis of the load-deformation response of uniformly heated steel beams obtained through transient state fire tests by considering the original beam cross-section properties and disregarding the changes in the cross-section areas under the applied loading; this model was thus assumed as an engineering stress-strain model in accordance with [17–20]. However, it should be emphasised that since the differences between the engineering and true stress-strain curves are very minor for strain values attained in the numerical simulations of steel beams in this study, which exhibit lateral-torsional buckling, the influence of the use of either engineering or true stress-strain response on the numerical results is expected to be immaterial. The stress-strain response of grade S355 steel determined through eq. (1) is shown in Fig. 2 for different elevated temperature levels.

The global geometric imperfections were assumed to be the lowest global buckling modes in shape and 1/1000 of the total member lengths in magnitude as shown in Fig. 3. Since the global LTB response of steel beams in fire is studied in this paper, the local imperfections were not incorporated into the finite element models. Unless otherwise indicated, fork-end support conditions, allowing warping deformations and rotations but restraining translations and twists, were adopted using the coupling constraint relationships at the beam ends. The ECCS [23] residual stress patterns for hot-rolled and welded I-sections shown in Fig. 4, where $f_{y,235} = 235$ MPa and f_y is the material yield stress, were applied to the finite element models of steel beams with hot-rolled and welded I-sections, respectively.

The finite element models were analysed isothermally using the following steps: (i) application of the residual stresses shown in Fig. 4 to the finite element models at room temperature, (ii) the incremental application of a uniform temperature increase to the models from room temperature to a predefined temperature value θ leading to the development of thermal strains in the models and the modification of their material response as shown in Fig. 2 and finally, (iii) application of the loading to the finite element models at the designated elevated temperature value θ . The first two steps were finalised only after reaching self-equilibrium in the models, while the modified Riks analysis [24, 25] were utilised in the last step to trace the full load-deformation response of a steel beam.

2.2. Validation of finite element models

The validation of the finite element models created in this study against the experiments carried out by Mesquita et al. [26] is provided in this subsection, where a series of tests on fork supported steel beams with a European IPE 100 cross-section and undergoing LTB at elevated temperatures were performed. The experiments were carried out under transient state conditions, whereby the beams were first loaded and then heated until their failure; the temperature value at which the failure was observed is referred to as the critical temperature θ_{cr} . The beams, whose lengths L varied between 1.5 m and 4.5 m, were heated uniformly by means of electroceramic mat elements, also employing a ceramic fibre mat to cover the specimens to improve the thermal efficiency. The heating was applied at a constant rate of 800 °C/h, which was controlled by a series of thermocouples attached to the specimens along their lengths. The specimens were subjected to three-point bending, where a concentrated load P was applied at the mid-span; the selfweight of the electroceramic mat elements, ceramic fibre mat and beam also created additional loading. Three tests were carried out for each beam length L by Mesquita et al. [26], using specimens with the same geometrical properties, loading conditions and the uniform 800 °C/h heating rate. The residual stresses, material properties and the mean value of the measured geometrical imperfections of the specimens reported by Mesquita et al. [26] were incorporated into the finite element models created herein, also considering the selfweight of the ceramic mat elements, beam and ceramic fibre mat. In Table 1, the critical temperature values determined through the finite element models $\theta_{cr,FE}$ are compared against those obtained from the experiments by [26] $\theta_{cr,test}$. As can be seen from the table, the finite element models provide critical temperature values $\theta_{cr,FE}$ in a good agreement with those obtained from the experiments $\theta_{cr,test}$, indicating that the finite element models created in this paper are able to replicate the response

of steel beams undergoing LTB at elevated temperatures. In all but one of the cases, the critical temperature values provided by the finite element models $\theta_{cr,FE}$ are slightly smaller than those obtained from the experiments. This was ascribed to the presence of the thermal insulation around the supports used within the experiments and the development of friction forces at the supports, generating additional axial restraints which reduced the deflections of the beams with the development of a catenary action as reported by Mesquita et al. [26]. The temperature versus mid-span vertical deflection paths of the specimens obtained from the experiments and the finite element models created herein are illustrated in Fig. 5 for beams with lengths L of 3.5 m and 4.5 m. As can be from the figure, the agreement between the temperature versus mid-span vertical deformation paths obtained from the experiments and finite element models is good, verifying that the finite element models created in this study are able to mimic the LTB response of steel beams in fire.

3. Existing design rules in EN 1993-1-2 for the LTB assessment of steel beams in fire

Prior to presenting key findings of the parametric studies, the design rules set out in EN 1993-1-2 [1] for the LTB assessment of steel beams in fire are briefly presented in this section. EN 1993-1-2 [1] provides the following equation for the determination of the design buckling resistance moment $M_{b,fi,t,Rd}$ of steel beams with Class 1 or Class 2 sections in fire at time t :

$$M_{b,fi,t,Rd} = \frac{\chi_{LT,fi} W_{pl,y} k_{y,\theta,com} f_y}{\gamma_{M,fi}}, \quad (5)$$

in which $\chi_{LT,fi}$ is the reduction factor for LTB in fire design situation, $k_{y,\theta,com}$ is the reduction factor for the yield strength of steel considering the maximum temperature in the compression flange $\theta_{a,com}$ reached at time t , $W_{pl,y}$ is the major axis plastic section modulus and $\gamma_{M,fi}$ is the partial factor for the yield strength for the fire situation, which is taken as unity (i.e. $\gamma_{M,fi} = 1.0$). The reduction factor for LTB in fire design situation $\chi_{LT,fi}$ is determined using the following equation:

$$\chi_{LT,fi} = \frac{1}{\phi_{LT,\theta,com} + \sqrt{\phi_{LT,\theta,com}^2 - \bar{\lambda}_{LT,\theta,com}^2}} \quad (6)$$

with

$$\phi_{LT,\theta,com} = 0.5 \left[1 + \eta_{LT} + \bar{\lambda}_{LT,\theta,com}^2 \right], \quad (7)$$

where η_{LT} is the generalised imperfection factor for the consideration of the influence of the geometric imperfections, residual stresses and spread of plasticity on the resistance of a steel beam in fire. EN 1993-1-2 [1] recommends the following expression for the determination of the generalised imperfection factor η_{LT} :

$$\eta_{LT} = \alpha \bar{\lambda}_{LT,\theta,com}, \quad (8)$$

in which α is the imperfection factor calculated as

$$\alpha = 0.65\sqrt{235/f_y}. \quad (9)$$

In eqs. (6), (7) and (8), the non-dimensional elevated temperature LTB slenderness $\bar{\lambda}_{LT,\theta,com}$ of a steel beam is determined through the following expression:

$$\bar{\lambda}_{LT,\theta,com} = \bar{\lambda}_{LT} \sqrt{\frac{k_{y,\theta,com}}{k_{E,\theta,com}}}, \quad (10)$$

where $k_{E,\theta,com}$ is the Young's modulus reduction factor at the maximum steel temperature in the compression flange $\theta_{a,com}$ reached at time t and $\bar{\lambda}_{LT}$ is the room temperature LTB slenderness of the beam determined by taking the square root of the ratio of the room temperature major axis plastic bending moment resistance $M_{y,pl}$ to the room temperature elastic buckling moment of a steel beam M_{cr} as shown below:

$$\bar{\lambda}_{LT} = \sqrt{\frac{M_{y,pl}}{M_{cr}}} = \sqrt{\frac{W_{pl,y}f_y}{M_{cr}}}. \quad (11)$$

Comparing the room temperature beam buckling design rules of EN 1993-1-1 [5] to the elevated temperature beam buckling design rules of EN 1993-1-2 [1], it can be observed that the elevated temperature beam buckling design rules of EN 1993-1-2 [1] are obtained through simple modifications to the beam buckling design formulae of [1] for the sake of establishing a consistency between EN 1993-1-1 [5] and EN 1993-1-2 [1]. In lieu of the room temperature yield strength f_y and the Young's modulus E_a , the elevated temperature yield strength $f_{y,\theta,com} = k_{y,\theta,com}f_y$ and Young's modulus $E_{a,\theta,com} = k_{E,\theta,com}E_a$ are used for the determination of the non-dimensional LTB slenderness $\bar{\lambda}_{LT,\theta,com}$, LTB buckling reduction factor $\chi_{LT,fi}$ and LTB resistance $M_{b,fi,Rd}$, thereby taking into account the erosion of the strength and stiffness on the LTB resistances of steel beams in fire. A specific generalised imperfection factor η_{LT} was also derived for the determination of $\chi_{LT,fi}$ on the basis of the results from GMNIA simulations as described in [7, 8]. The use of the elevated temperature slenderness $\bar{\lambda}_{LT,\theta,com}$ in eq. (6) obtained through the multiplication of the room temperature LTB slenderness $\bar{\lambda}_{LT}$ by a factor of $\sqrt{k_{y,\theta,com}/k_{E,\theta,com}}$ (i.e. $\bar{\lambda}_{LT,\theta,com} = \bar{\lambda}_{LT}\sqrt{k_{y,\theta,com}/k_{E,\theta,com}}$), which is greater than unity for the majority of the elevated temperature values typically considered in the fire design of steel structures as shown in Fig. 6, enables the consideration of the increased susceptibility of a steel beam to LTB in fire owing to the more rapid reduction of the Young's modulus E_a relative to the yield strength f_y for carbon steel at elevated temperatures (see Fig. 1).

Despite their calibration against the results from the nonlinear finite element simulations of steel beams, the LTB assessment equations of EN 1993-1-2 [1] are based on a somewhat limited number of cases taken into consideration in [7] as also indicated by [8], considering the LTB response of only IPE 220 beams in fire and thus disregarding the influence of the cross-section shapes on the elevated temperature LTB response of steel beams. Moreover,

recent studies [4, 27] have pointed out a somewhat low degree of accuracy of the current room temperature EN 1993-1-1 [5] beam buckling design rules when they are compared against the results obtained from the GMNIA simulations of beams with different cross-section shapes. This rather low degree of accuracy of the room temperature LTB design rules of [5] was ascribed to these design formulae employing the Perry-Robertson equation developed considering the flexural buckling response of steel columns to determine the LTB buckling reduction factors by simply changing the flexural buckling slenderness to the LTB slenderness and thus their inability to provide a sound representation of the mechanical response of steel beams undergoing LTB. Since the elevated temperature beam buckling design rules of EN 1993-1-2 [1] are derived through simple modifications to the room temperature beam buckling design rules, it is expected that they may have similar shortcomings.

In the following section, the accuracy of EN 1993-1-2 [1] beam buckling rules is assessed considering different parameters and their shortcomings are identified. New design rules are introduced in Section 5 with the aim of providing a design approach eliminating the shortcomings of the current LTB assessment rules of EN 1993-1-2 [1].

4. Parametric studies

This section addresses a series of key findings of the parametric studies performed in this paper. A summary of the performed parametric studies is provided in Table 2, showing that (i) twelve European cross-section shapes with varying proportions and different levels of susceptibility to LTB, (ii) three commonly used steel grades (i.e. S235, S355, S460), (iii) different fabrication processes (i.e. welded beams, hot-rolled beams), (iii) four different elevated temperature levels 200 °C, 400 °C, 600 °C, 800 °C and (v) ten different elevated temperature non-dimensional LTB slendernesses $\bar{\lambda}_{LT,\theta}$ ranging between 0.2 and 2.0 with increments in $\bar{\lambda}_{LT,\theta}$ of 0.2 were considered. All of the parameters provided in Table 2 were taken into consideration for each cross-section shape, resulting in 240 GMNIA simulations for each cross-section type and a total of 2832 GMNIA simulations of the LTB response of steel beams in fire. In the case of beams with an HEM 200 cross-section, the LTB non-dimensional slenderness values $\bar{\lambda}_{LT,\theta}$ ranging between 0.2 and 1.6 with increments in $\bar{\lambda}_{LT,\theta}$ of 0.2 were taken into consideration as the beams with $\bar{\lambda}_{LT,\theta} > 1.6$ have the length L to cross-section depth h ratios L/h lie significantly beyond the range likely to be used in practice. Since the beams were uniformly heated, their elevated temperature slenderness $\bar{\lambda}_{LT,\theta}$ were determined by multiplying their room temperature LTB slenderness by a factor of $\sqrt{k_{y,\theta}/k_{E,\theta}}$ (i.e. $\bar{\lambda}_{LT,\theta} = \bar{\lambda}_{LT} \sqrt{k_{y,\theta}/k_{E,\theta}}$). It should be noted that a small number of cross-sections considered in the parametric studies, which are presented in Table 2, fall into the Class 3 and 4 categories according to the cross-section classification approach of EN 1993-1-2 [1]. However, since local imperfections were not incorporated into the finite element models, the steel beams with these cross-sections are susceptible to global buckling effects. These cross-sections were included in the parametric studies for the purpose of verifying the accuracy of the proposed method in the global buckling assessment of steel beams with a broad range of cross-section properties. Future research will be directed towards the extension of the proposed design approach for the consideration of combined global and

local buckling effects for beams with Class 3 and 4 sections.

4.1. Influence of the cross-section shape on the LTB response of a steel beam in fire

The influence of the cross-section shape on the LTB response of steel beams in fire is illustrated in Fig. 7, considering three cross-section shapes IPE 500, IPE 80 and HEM 200, which represent slender, moderately slender and stocky beam cross-sections, different elevated temperature levels and various non-dimensional LTB slendernesses $\bar{\lambda}_{LT,\theta}$. As can be seen from Fig. 7, the cross-section shape has a rather significant influence on the elevated temperature LTB strengths of steel beams in that the stockier the beam cross-section, the lower the susceptibility of a steel beam in fire. Fig. 7 shows that the LTB strength of a steel beam normalised by the elevated temperature plastic cross-section resistance $M_{y,Ed}/(W_{pl,y}k_{y,\theta}f_y)$ becomes greater for stockier sections even for the same value of the elevated temperature non-dimensional LTB slenderness $\bar{\lambda}_{LT,\theta}$, indicating that an adjustment to an LTB design curve considering the shape of a beam cross-section is necessary to enable accurate ultimate strength predictions. The accuracy of the current LTB assessment rules of EN 1993-1-2 [1] is also assessed in Fig. 7. As can be seen from the figure, the current beam buckling rules of EN 1993-1-2 fails to accurately recognise the influence of the cross-section shape on the susceptibility of a steel beam to LTB in fire and provide a single LTB curve, which indicates that the accuracy of the current LTB assessment rules provided in EN 1993-1-1 [1] can be enhanced by modifying the design formulae for the consideration of the influence of the cross-section shapes on LTB design curves.

4.2. Influence of the grade of steel on the LTB response of a steel beam in fire

In Fig. 8, the effect of the grade of steel on the LTB behaviour of steel beams in fire is shown for steel beams with hot-rolled IPE 500 section, considering grade S235, S355 and S460 steel, different elevated temperature levels and LTB slendernesses $\bar{\lambda}_{LT,\theta}$. As can be seen from the figure, the higher the grade of steel, the greater the normalised elevated temperature LTB strength of a beam $M_{y,Ed}/(W_{pl,y}k_{y,\theta}f_y)$ for the same elevated temperature LTB slenderness $\bar{\lambda}_{LT,\theta}$, suggesting that an LTB design curve should be modified considering the grade of steel to achieve a high level of accuracy in the estimations of the LTB strengths of steel beams in fire. The accuracy of the current LTB design rules of EN 1993-1-2 [1] is also illustrated in Fig. 8, where it can be seen that the LTB equations of EN 1993-1-2 consider the influence of the grade of steel on the LTB reduction factor $\chi_{LT,fi}$ by defining the imperfection factor α as a function of the yield strength $\alpha = 0.65\sqrt{235/f_y}$ as shown in eq. (9), leading to LTB curves providing greater ultimate strength predictions for higher steel grades. The consideration of the influence of the grade of steel on the LTB resistances of steel beams in fire results in an improved level of accuracy of EN 1993-1-2 [1] design rules as shown in Fig. 8, though there is still room for improvement of the accuracy of the EN 1993-1-2 [1] rules, which lead to the overpredictions of the ultimate strengths in some cases for the considered IPE 500 beams.

4.3. Influence of residual stresses on the LTB response of a steel beam in fire

The high influence of residual stresses on the room temperature LTB strengths of steel beams has been shown in previous studies [28–30]. In this subsection, the influence of

residual stresses on the elevated temperature LTB strengths of steel beams is investigated. Fig. 9 shows a comparison of the LTB strengths of hot-rolled and welded IPE 500 steel beams with the different residual stress patterns shown in Fig. 4 in addition to the LTB strengths of steel beams free from residual stresses, considering the elevated temperature levels $T = 200$ °C, 400 °C, 600 °C, 800 °C and different non-dimensional LTB slendernesses $\bar{\lambda}_{LT,\theta}$. As can be seen from Fig. 9, while residual stresses significantly affect the ultimate strengths of steel beams at the elevated temperature level of $T = 200$ °C, the influence of residual stresses on the LTB strengths of steel beams becomes low for the elevated temperature values of $T = 400$ °C, 600 °C, 800 °C. This low influence of the residual stresses on the LTB strengths results from the dissipation of the residual stresses within steel beams with increasing elevated temperature levels as a result of the development of thermal strains. This is shown in Fig. 10, where the finite element models of steel beams are uniformly heated up to different elevated temperature levels following the application of the residual stresses. As can be seen from the figure, the higher the elevated temperature level, the lower the residual stresses. The findings of this subsection indicates that separate LTB design rules for hot-rolled and welded steel beams in fire is not necessary. This is recognised in the LTB assessment rules of EN 1993-1-2 [1], where the LTB design curves are not modified on the basis of the fabrication process of a steel beam as shown in Fig. 9. Low influence of residual stresses on the LTB strengths of steel beams at elevated temperatures was also observed in Franssen [31] and Vila Real et al. [32].

4.4. Influence of elevated temperature level on the LTB response of a steel beam in fire

As a final key finding of the parametric studies carried out in this paper, the influence of the elevated temperature level on the LTB strengths of steel beams in fire is presented in this subsection. The influence of the elevated temperature level on the resistances of steel beams is, of course, accounted for through the reduction of the yield strength $f_{y,\theta} = k_{y,\theta} f_y$ in the determination of their ultimate strengths. Herein, the influence of the elevated temperature levels on the normalised elevated temperature LTB strengths $M_{y,Ed}/(W_{pl,y} k_{y,\theta} f_y)$ is investigated so as to assess whether a modification of a fire LTB design curve is necessary to obtain different buckling reduction factors $\chi_{LT,fi}$ for the same elevated temperature LTB slenderness $\bar{\lambda}_{LT,\theta}$ at different elevated temperature levels. The influence of the elevated temperature level on the normalised LTB strengths of steel beams $M_{y,Ed}/(W_{pl,y} k_{y,\theta} f_y)$ in fire is shown in Fig. 11. As can be seen from the figure, even though there are significant reductions of the normalised elevated temperature LTB strengths when the temperature is increased from $T = 200$ °C to $T = 400$ °C, the differences between the normalised elevated temperature LTB strengths $M_{y,Ed}/(W_{pl,y} k_{y,\theta} f_y)$ become low for the elevated temperature values of $T = 400$ °C, 600 °C and 800 °C. Fig. 11 shows that EN 1993-1-2 [1] recognises the small influence of an elevated temperature level on the normalised LTB strengths of steel beams $M_{y,Ed}/(W_{pl,y} k_{y,\theta} f_y)$, providing a single buckling curve regardless of the elevated temperature level, though the ultimate strengths of the beams are overestimated in some cases.

As can be seen from the results presented in this section, the current LTB design rules of EN 1993-1-2 [1] have a series of shortcomings, highlighting the scope for improvement

of their accuracy. One of the most prominent shortcomings of these design rules is their failure to recognise the necessity of the adjustment to the LTB curves for different beam cross-section shapes with different levels of susceptibility to LTB, which results in a rather low level of accuracy for beams with cross-sections having properties significantly different than those of the IPE 220 section considered during the development of the EN 1993-1-2 [1] LTB design rules [7]. For the purpose of achieving an improved accuracy in the elevated temperature LTB design rules of steel beams, the Perry-Robertson equation of Taras and Greiner [4] able to provide a sound representation of the LTB response of steel beams at room temperature is adopted for the design of steel beams against LTB at elevated temperatures in the following section, which is also calibrated against a large a number of GMNIA results of steel beams considering a broad range of parameters shown in Table 2.

5. Development of new design rules for the LTB assessment of steel beams in fire

In this section, new design rules for the LTB assessment of steel beams in fire are developed. Initially, the adoption of the Perry-Robertson equation originally derived by Taras and Greiner [4] for the representation of the LTB response of an imperfect elastic steel beam in fire is provided. Following the presentation of the new Perry-Robertson equation, its calibration against the results from shell finite element models is illustrated. In line with the approach followed in the development of the column buckling design proposals of Franssen et al. [33, 34], which have been adopted as the column buckling design rules of EN 1993-1-2 [1], the elevated temperature range of 400 °C to 800 °C was considered in the development of the beam buckling design equations in this section.

5.1. Adoption of the Perry-Robertson equation of Taras and Greiner [4] for the representation of the LTB response of steel beams in fire

Assuming a uniform temperature increase within an imperfect elastic steel beam under constant bending, resulting in uniform reductions of the yield strength $f_{y,\theta} = k_{y,\theta}f_y$ and Young's modulus $E_{a,\theta} = k_{E,\theta}E_a$, a Perry-Robertson equation representing the LTB failure of the beam in fire can be derived by taking into account the internal forces within its most heavily loaded mid-span section as illustrated in Fig. 12 and considering the failure on the basis of the first yield criterion through the following expression:

$$\frac{M_y}{W_{el,y}k_{y,\theta}f_y} + \frac{M_z^{II}}{W_{el,z}k_{y,\theta}f_y} + \frac{M_w^{II}}{I_wk_{y,\theta}f_y} \frac{bh}{4} = 1.0 \quad (12)$$

where M_y is the major axis bending moment applied to the fork-end supported beam, $W_{el,y}$ is the minor axis elastic section modulus, I_w is the warping constant, b and h are the flange width and cross-section depth and M_z^{II} and M_w^{II} are the second-order minor axis bending moment and warping moment at the mid-span section, respectively. Assuming the geometric imperfection of the beam its lowest eigenmode in shape where \bar{u}_0 and $\bar{\phi}_0$ are the magnitudes of the initial lateral translation and twist at the mid-span section, the second-order minor

axis bending moment M_z^{II} and the warping moment M_w^{II} at the mid-span section can be expressed as shown below:

$$M_z^{II} = \bar{\phi}_0 \frac{M_y}{1 - M_y/M_{cr,\theta}} \quad (13)$$

$$M_w^{II} = \frac{N_{cr,z,\theta}}{M_{cr,\theta}} \frac{I_w}{I_z} \bar{\phi}_0 \frac{M_y}{1 - M_y/M_{cr,\theta}} \quad (14)$$

in which I_z is the second moment of area about the minor axis and $M_{cr,\theta}$ and $N_{cr,z,\theta}$ are the elastic buckling moment and minor axis flexural buckling load of a beam at temperature θ calculated as:

$$M_{cr,\theta} = \frac{\pi^2 k_{E,\theta} E_a I_z}{L^2} \sqrt{\frac{I_w}{I_z} + \frac{k_{E,\theta} G_a I_t L^2}{\pi^2 k_{E,\theta} E_a I_z}} = k_{E,\theta} M_{cr}, \quad (15)$$

$$N_{cr,z,\theta} = \frac{\pi^2 k_{E,\theta} E_a I_z}{L^2} = k_{E,\theta} N_{cr,z}, \quad (16)$$

where M_{cr} and $N_{cr,z}$ are the elastic buckling moment and minor axis flexural buckling load of the beam at room temperature, L is the length of the beam, G_a is the shear modulus and I_t is the torsion constant. It should be noted the detailed description of the derivation of M_z^{II} and M_w^{II} is provided in [4], which also applies to the considered case herein with the use of $M_{cr,\theta}$ and $N_{cr,z,\theta}$ in lieu of M_{cr} and $N_{cr,z}$ owing to the assumption of a uniform temperature increase within the steel beam. The maximum geometric imperfection in the beam \bar{e}_0 can be expressed as (see Fig. 12):

$$\bar{e}_0 = \bar{u}_0 + \frac{h}{2} \bar{\phi}_0. \quad (17)$$

Since the geometric imperfection of the beam is assumed its lowest eigenmode in shape, the following relationship between the initial lateral translation \bar{u}_0 and twist $\bar{\phi}_0$ at the mid-span section can be written as [4]:

$$\bar{u}_0 = \bar{\phi}_0 \frac{M_{cr,\theta}}{N_{cr,z,\theta}}. \quad (18)$$

Using the expression provided by eq. (18) to define \bar{u}_0 in eq. (17), $\bar{\phi}_0$ can be expressed in terms of \bar{e}_0 as follows:

$$\bar{\phi}_0 = \frac{\bar{e}_0}{M_{cr,\theta}/N_{cr,z,\theta} + h/2}. \quad (19)$$

Substituting eq. (13), eq. (14) and eq. (19) into eq. (12) results in the following equation:

$$\frac{M_y}{W_{el,y} k_{y,\theta} f_y} + \frac{M_y}{W_{el,z} k_{y,\theta} f_y} \left(\frac{1}{1 - M_y/M_{cr,\theta}} \right) \left(\frac{\bar{e}_0}{M_{cr,\theta}/N_{cr,z,\theta} + h/2} \right) \left(1 + \frac{N_{cr,z,\theta} h}{M_{cr,\theta} 2} \right) = 1.0 \quad (20)$$

Multiplying the second part of the equation on the left hand side by A/A and $W_{el,y}/W_{el,y}$, the equation below is obtained:

$$\frac{M_y}{W_{el,y}k_{y,\theta}f_y} + \frac{M_y}{W_{el,y}k_{y,\theta}f_y} \left(\frac{1}{1 - M_y/M_{cr,\theta}} \right) \left(\frac{A\bar{e}_0}{W_{el,z}} \right) \left(\frac{W_{el,y}}{A} \right) \left(\frac{N_{cr,z,\theta}}{M_{cr,\theta}} \right) = 1.0. \quad (21)$$

The reduction factor for LTB in fire $\chi_{LT,fi}$ and the non-dimensional elevated temperature LTB slenderness $\bar{\lambda}_{LT,\theta}$ and minor axis flexural buckling slenderness $\bar{\lambda}_{z,\theta}$ can be expressed as:

$$\chi_{LT,fi} = \frac{M_y}{W_{el,y}k_{y,\theta}f_y}, \quad \bar{\lambda}_{LT,\theta} = \sqrt{\frac{W_{el,y}k_{y,\theta}f_y}{M_{cr,\theta}}}, \quad \bar{\lambda}_{z,\theta} = \sqrt{\frac{Ak_{y,\theta}f_y}{N_{cr,z,\theta}}}. \quad (22)$$

Employing the expressions for $\chi_{LT,fi}$, $\bar{\lambda}_{LT,\theta}$ and $\bar{\lambda}_{z,\theta}$ given by eq. (22), eq. (21) can be written as:

$$\chi_{LT,fi} + \chi_{LT,fi} \frac{1}{1 - \chi_{LT,fi}\bar{\lambda}_{LT,\theta}^2} \frac{A\bar{e}_0}{W_{el,z}} \frac{\bar{\lambda}_{LT,\theta}^2}{\bar{\lambda}_{z,\theta}^2} = 1.0. \quad (23)$$

Expressing eq. (23) in terms of $\chi_{LT,fi}$ yields:

$$\chi_{LT,fi} = \frac{1}{\phi_{LT,\theta} + \sqrt{\phi_{LT,\theta}^2 - \bar{\lambda}_{LT,\theta}^2}}$$

with $\phi_{LT,\theta} = 0.5 \left[1 + \eta_{LT} \frac{\bar{\lambda}_{LT,\theta}^2}{\bar{\lambda}_{z,\theta}^2} + \bar{\lambda}_{LT,\theta}^2 \right],$ (24)

where η_{LT} is the generalised imperfection factor equal to:

$$\eta_{LT} = \frac{A\bar{e}_0}{W_{el,z}}. \quad (25)$$

The format of eq. (24) is the same as that of the Perry-Robertson equation derived by Taras and Greiner [4] with the exception of the presence of the elevated temperature slendernesses $\bar{\lambda}_{LT,\theta}$ and $\bar{\lambda}_{z,\theta}$ in lieu of their room temperature counterparts $\bar{\lambda}_{LT}$ and $\bar{\lambda}_z$, which enables the increased susceptibility of a steel beam to LTB in fire to be taken into consideration as $\bar{\lambda}_{LT,\theta} \geq \bar{\lambda}_{LT}$ and $\bar{\lambda}_{z,\theta} \geq \bar{\lambda}_z$. It should be emphasised that the factor $\bar{\lambda}_{LT,\theta}^2/\bar{\lambda}_{z,\theta}^2$ is the key parameter in eq. (24) which accounts for the susceptibility of a beam cross-section to LTB by modifying the generalised imperfection factor η_{LT} and thus $\chi_{LT,fi}$ for a particular value of $\bar{\lambda}_{LT,\theta}$, thereby leading to a particular LTB buckling curve for each beam cross-section shape. The parameter $\bar{\lambda}_{LT,\theta}^2/\bar{\lambda}_{z,\theta}^2$, which does not exist in the Perry-Robertson equation adopted in EN 1993-1-2 [1] as can be seen in Section 3, is of pivotal importance for the accurate calibration of the Perry-Robertson equation given by eq. (24), which has been previously shown in [4, 14, 35]. In the following subsection, the calibration of eq. (24) against a large number of results obtained from the GMNIA of the finite element models considering a wide range of cross-section shapes, elevated temperature values and member slendernesses is presented.

5.2. Calibration of the Perry-Robertson equation for the representation of the LTB response of steel beams in fire

Similar to the approach adopted in [14, 35], the LTB equation given by eq. (24) is calibrated by comparing the generalised imperfection factor η_{LT} to those obtained through FE modelling $\eta_{LT,FE}$. The generalised imperfection factor from FE modelling $\eta_{LT,FE}$ is obtained rearranging eq. (24) in terms of η_{LT} , which gives the following expression:

$$\eta_{LT,FE} = \frac{1 - \chi_{LT,fi,FE}}{\chi_{LT,fi,FE}} \left(1 - \chi_{LT,fi,FE} \bar{\lambda}_{LT,\theta}^{-2} \right) \left(\frac{\bar{\lambda}_{z,\theta}^{-2}}{\bar{\lambda}_{LT,\theta}^{-2}} \right), \quad (26)$$

where $\chi_{LT,fi,FE}$ is the ratio of the ultimate strength of the steel beam obtained from the GMNIA to the plastic bending moment capacity $M_{y,pl}$. Note that in the calibration of eq. (24), the elevated temperature LTB slenderness determined considering the plastic bending moment resistance of the beam cross-section $\bar{\lambda}_{LT,\theta} = \sqrt{W_{pl,y} k_{y,\theta} f_y / M_{cr,\theta}}$ was used in accordance with [4]. Moreover, the expression of the generalised imperfection η_{LT} provided in eq. (25) and derived considering the elastic LTB response of steel beams was changed to consider the influence of the plasticity, residual stresses and geometrical imperfections on the LTB resistances of steel beams in fire in line with [36, 37]. Employing eq. (26), eq. (24) was calibrated to the GMNIA results for a number of fork-end supported beams considering twelve cross-section shapes shown in Table 2. For each cross-section, grades S235, S355 and S460 steel, the elevated temperature levels of 400 °C, 600 °C and 800 °C (i.e. $T = 400$ °C, 600 °C, 800 °C) and non-dimensional LTB slenderness $\bar{\lambda}_{LT,\theta}$ ranging between 0.2 and 2.0 with increments in $\bar{\lambda}_{LT,\theta}$ of 0.2 were taken into consideration. As put forward by Taras and Greiner [4], the multiplication of η_{LT} by an additional cross-section factor $\sqrt{W_{el,y}/W_{el,z}}$, where $W_{el,y}$ and $W_{el,z}$ are the elastic section moduli about the major and minor axis, results in a more accurate calibration, which was also adopted in this paper. Moreover, as illustrated in Fig. 8, the higher the steel grade, the higher the LTB buckling curves, which is accounted for in EN 1993-1-2 [1] by multiplying the imperfection factor α by a factor of $\sqrt{235/f_y}$. This approach was also adopted in this study. With these improvements, the accuracy of the proposed calibrated expressions of η_{LT} relative to $\eta_{LT,FE}$ is illustrated in Fig. 13 for S235, S355 and S460 grades considering the elevated temperature levels of 400 °C, 600 °C and 800 °C and hot-rolled and welded steel beams. In line with [4], it was observed herein that the expression of the generalised imperfection factor η_{LT} as a function of the room temperature minor axis flexural buckling slenderness $\bar{\lambda}_z$ leads to a very accurate calibration. Moreover, a lower bound of $\eta_{LT,lim} = 1.15\sqrt{235/f_y}\bar{\lambda}_z$ was also defined for η_{LT} (i.e. $\eta_{LT} \leq \eta_{LT,lim} = 1.15\sqrt{235/f_y}\bar{\lambda}_z$) to avoid significant overestimations of the LTB strengths of beams with stocky sections.

It should be emphasised that the definition of the generalised imperfection factor η_{LT} as a function of the room temperature minor axis flexural slenderness $\bar{\lambda}_z$ (e.g. $\eta_{LT} = 0.45\sqrt{W_{el,y}/W_{el,z}}\bar{\lambda}_z$) in lieu of either the elevated temperature LTB $\bar{\lambda}_{LT,\theta}$ or minor axis $\bar{\lambda}_{z,\theta}$ slenderness obviates the dependency of the generalised imperfection factor η_{LT} on the elevated temperature levels and makes it directly proportional to the beam lengths, thereby

enabling a consistent consideration of imperfections existing in steel beams which are typically not influenced by elevated temperature levels and defined as directly proportional to the member lengths according to the fabrication tolerances as given in EN 1090-2 [38]. The higher accuracy and consistency of the definition of the generalised imperfection factor in a Perry-Robertson equation as a function of room temperature flexural buckling slenderness are recently shown in Kucukler et al. [39] for stainless steel columns undergoing flexural buckling in fire, for which it was illustrated that the definition of the generalised imperfection factor as a function of the elevated temperature flexural buckling slenderness leads to quite inaccurate strength estimations. It is also worth noting that the generalised imperfection factor is defined as a function of the minor axis flexural buckling slenderness $\bar{\lambda}_z$ in the LTB assessment equations that will appear in the upcoming version of the room temperature European structural steel design standard EN 1993-1-1 [5], which is currently referred to as prEN 1993-1-1 [6], thus the proposal made herein for the definition of η_{LT} also brings about consistency with the new room temperature LTB assessment rules of EN 1993-1-1 [5]. Fig. 13 shows that the accuracy of the calibrated expression of the generalised imperfection factor provided in eq. (27) is high.

$$\eta_{LT} = 0.45 \sqrt{\frac{W_{el,y}}{W_{el,z}}} \sqrt{\frac{235}{f_y}} \bar{\lambda}_z \geq 1.15 \sqrt{\frac{235}{f_y}} \bar{\lambda}_z \quad (27)$$

In the following subsection, the final format of the proposed design rules for LTB assessment of steel beams in fire is provided.

5.3. Proposed design rules for LTB assessment of steel beams in fire

The following expression is recommended for the determination of the design buckling resistance moment of steel beams $M_{b,fi,t,Rd}$ with Class 1 or Class 2 sections in fire at time t

$$M_{b,fi,t,Rd} = \frac{\chi_{LT,fi} W_{pl,y} k_{y,\theta,com} f_y}{\gamma_{M,fi}}, \quad (28)$$

where $k_{y,\theta,com}$ is the reduction factor for the yield strength of steel considering the maximum temperature in the compression flange $\theta_{a,com}$ reached at time t , $W_{pl,y}$ is the major axis plastic section modulus and $\gamma_{M,fi}$ is the partial factor for the yield strength for the fire situation, which is taken as unity (i.e. $\gamma_{M,fi} = 1.0$). It should be noted that the new beam buckling design rules were developed considering a uniform temperature increase within steel beams as can be seen in Subsection 5.1 and Subsection 5.2 similar to the approach adopted in the development of the EN 1993-1-2 [1] beam buckling design rules [7] and expected to lead to safe results when the maximum temperature within the compression flange $\theta_{a,com}$ is taken into consideration if temperature varies across the steel beam. The LTB reduction factor in fire design situation $\chi_{LT,fi}$ is calculated using the following equation:

$$\chi_{LT,fi} = \frac{1}{\phi_{LT,\theta,com} + \sqrt{\phi_{LT,\theta,com}^2 - \bar{\lambda}_{LT,\theta,com}^2}} \quad (29)$$

with

$$\phi_{LT,\theta,com} = 0.5 \left[1 + \eta_{LT} \frac{\bar{\lambda}_{LT,\theta,com}^2}{\bar{\lambda}_{z,\theta,com}^2} + \bar{\lambda}_{LT,\theta,com}^2 \right], \quad (30)$$

where $\bar{\lambda}_{z,\theta,com}$ is the minor axis flexural buckling slenderness of a steel beam determined as:

$$\bar{\lambda}_{z,\theta,com} = \bar{\lambda}_z \sqrt{\frac{k_{y,\theta,com}}{k_{E,\theta,com}}}, \quad (31)$$

in which $k_{E,\theta,com}$ is the Young's modulus reduction factor at the maximum steel temperature in the compression flange $\theta_{a,com}$ reached at time t and $\bar{\lambda}_z$ is the room temperature flexural buckling slenderness calculated as:

$$\bar{\lambda}_z = \sqrt{\frac{Af_y}{N_{cr,z}}} \quad (32)$$

where A is the cross-section area of the beam and $N_{cr,z}$ is the room temperature minor axis flexural buckling load. In eqs. (29) and (30), the non-dimensional elevated temperature LTB slenderness $\bar{\lambda}_{LT,\theta,com}$ of a steel beam is determined through the following expression:

$$\bar{\lambda}_{LT,\theta,com} = \bar{\lambda}_{LT} \sqrt{\frac{k_{y,\theta,com}}{k_{E,\theta,com}}}, \quad (33)$$

where $\bar{\lambda}_{LT}$ is the room temperature LTB slenderness of the beam calculated by taking the square root of the ratio of the room temperature major axis plastic bending moment resistance $M_{y,pl}$ to the room temperature elastic buckling moment of a steel beam M_{cr} :

$$\bar{\lambda}_{LT} = \sqrt{\frac{M_{y,pl}}{M_{cr}}} = \sqrt{\frac{W_{pl,y}f_y}{M_{cr}}}. \quad (34)$$

The generalised imperfection factor is determined using the following expression:

$$\eta_{LT} = \alpha_{LT} \sqrt{\frac{235}{f_y}} \bar{\lambda}_z, \quad (35)$$

in which α_{LT} is the imperfection factor determined as:

$$\alpha_{LT} = 0.45 \sqrt{\frac{W_{el,y}}{W_{el,z}}} \geq 1.15. \quad (36)$$

Comparing the existing beam buckling design rules to those proposed in this paper, it can be seen that the proposed design rules do not bring about an increased complexity and involve the additional factor $\bar{\lambda}_{LT,\theta,com}^2/\bar{\lambda}_{z,\theta,com}^2$ which enables a more accurate estimation of the LTB response of steel beams in fire. In the following section, the accuracy of the proposed LTB assessment design rules for steel beams in fire is investigated.

6. Assessment of the accuracy of the proposed design rules against the existing design rules in EN 1993-1-2 for LTB assessment of steel beams in fire

In this section, the accuracy and reliability of the proposed LTB assessment design rules for steel beams in fire are investigated. As discussed in Section 4, one of the most prominent shortcomings of the current LTB assessment design rules of EN 1993-1-2 [1] is their inability to accurately account for the influence of the cross-section shape on the LTB strengths of steel beams. In Fig. 14, the accuracy of the new design rules is assessed for steel beams with IPE 500, IPE 80 and HEM 200 sections, representing slender, moderately slender and stocky beam cross-sections. Fig. 14 shows that the beam buckling design rules proposed in this paper lead to quite accurate ultimate strength predictions for steel beams in fire with different cross-section shapes. Comparing Fig. 14 to Fig. 7, it can be observed that the proposed beam buckling design method provides more accurate ultimate strength predictions relative to the existing LTB assessment design rules of EN 1993-1-2 [1] owing to its accurate consideration of the influence of the beam cross-sections on the LTB resistances of steel beams in fire.

In addition to the beams shown in Fig. 14, the accuracy of the proposed design method is also compared against that of the existing beam buckling design rules of EN 1993-1-2 [1] in Table 3 for steel beams with the twelve cross-section shapes illustrated in Table 2, considering the elevated temperature levels of 400 °C, 600 °C and 800 °C (i.e. $T = 400$ °C, 600 °C and 800 °C), grades S235, S355 and S460 and the elevated temperature non-dimensional slendernesses $\bar{\lambda}_{LT,\theta}$ ranging between 0.2 and 2.0 with increments in $\bar{\lambda}_{LT,\theta}$ of 0.2. In Table 3, N is the number of the considered steel beams, ϵ is the ratio of the ultimate resistance of the beam obtained from the GMNIA R_{GMNIA} to that determined through the corresponding design method R_{method} (i.e. $\epsilon = R_{GMNIA}/R_{method}$) and ϵ_{av} , ϵ_{COV} , ϵ_{max} and ϵ_{min} are the average, coefficient of variation (COV), maximum and minimum of the ϵ values respectively. Thus, an ϵ value smaller than 1.0 indicates an unsafe ultimate strength prediction of a design method. As can be seen from Table 3, the proposed LTB assessment design rules for steel beams in fire bring about an improved accuracy relative to the existing beam buckling design methods of EN 1993-1-2 [1] with lower ϵ_{COV} values.

The reliability of the proposed design method and that of the beam buckling design rules of EN 1993-1-2 [1] are also assessed in Table 4 considering the three reliability criteria proposed by Kruppa [40] for the fire design of structural steel elements. Criterion 1 of [40] states that none of the strength predictions R_{method} should exceed the FE results R_{GMNIA} by more than 15% (i.e. $(R_{method} - R_{GMNIA})/R_{GMNIA} \leq 15\%$). Criterion 2 states that less than 20% of the design predictions should be on the unsafe side, i.e. $num(R_{method} > R_{GMNIA})/num(R_{GMNIA} \leq 20\%)$. Finally, Criterion 3 states that the design predictions should be safe-sided on average, i.e. $\bar{X}[(R_{method} - R_{GMNIA})/R_{GMNIA}] < 0\%$. As can be seen from Table 4, the proposed design method fulfils all three reliability criteria put forward by [40]. On the other hand, the beam buckling design rules of EN 1993-1-2 [1] fail to satisfy the Criterion 1 and Criterion 2 of [40].

The accuracy of the proposed beam buckling design rules is also visually illustrated against that of the existing LTB assessment rules of EN 1993-1-2 [1] in Fig. 15 and Fig. 16

for hot-rolled and welded steel beams with the twelve cross-section shapes shown in Table 2, considering the elevated temperature levels of 200 °C, 400 °C, 600 °C and 800 °C, grades S235, S355 and S460 steel and $\bar{\lambda}_{LT,\theta}$ ranging between 0.2 and 2.0 with increments in $\bar{\lambda}_{LT,\theta}$ of 0.2. As can be seen in Fig. 15 and Fig. 16, the proposed design method leads to more accurate and safe ultimate strength predictions relative to the existing beam buckling rules of EN 1993-1-2 [1], while both the proposed method and EN 1993-1-2 [1] provide safe LTB strength predictions for beams for the elevated temperature level of 200 °C.

In accordance with the observations made in this study, Vila Real et al. [8] also concluded that the combined influence of the beam cross-section depth-to-width ratio (i.e. h/b), the residual stress pattern, which changes for hot-rolled and welded sections as shown in Fig. 4, and the steel grade may be of importance for the LTB response of steel beams in fire. These factors were readily considered in the LTB design equations proposed by Vila Real et al. [8] by simple modifications to the existing LTB design equations in EN 1993-1-2 [1], which provided a higher level of safety relative to the EN 1993-1-2 [1] LTB assessment equations and enabled the consistency with the design equations provided for the room temperature LTB assessment of steel beams in EN 1993-1-1 [5]. The accuracy and reliability of the design method proposed by Vila Real et al. [8] for the LTB assessment of steel beams in fire are also shown in Table 3 and Table 4, respectively. It can be seen from Table 4 that the design method proposed by Vila Real et al. [8] leads to an improved level of reliability relative to the existing LTB assessment method provided in EN 1993-1-2 [1]. The LTB design equations of [8] only slightly violate the Criterion 2 of Kruppa [40], which can be deemed to be acceptable, and satisfy the other reliability criteria of [40].

It should be noted that similar to the EN 1993-1-2 [1] column design rules, which were developed considering the buckling response of steel columns at the elevated temperature range of 400 °C to 800 °C [33, 34], the proposed design equations can be safely applied for temperature values T higher than 800 °C (i.e. $T > 800$ °C) and lower than 400 °C ($T < 400$ °C) in line with the scope of applicability of the column buckling design rules of [1] as indicated by [33, 34]. For $T < 400$ °C and $T > 800$ °C, a carbon steel member exhibits a lower susceptibility to instability relative to its structural response within the elevated temperature range of 400 °C $\leq T \leq 800$ °C with lower $\bar{\lambda}_{LT,\theta}$ values as illustrated in Fig. 6.

Finally, it is worth noting that in accordance with the recommendations of Franssen et al. [33, 34], the following approach can be adopted to obtain more accurate and less conservative LTB strength predictions for steel beams with temperature values T lower than 400 °C: (i) determine the ultimate LTB strength of a steel beam at 100 °C using the room temperature LTB design rules provided in prEN 1993-1-1 [5], which is the same as its ultimate LTB strength at room temperature 20 °C, (ii) calculate the ultimate LTB strength of the beam at 400 °C using the proposed LTB design equations in this paper and finally (iii) determine the actual LTB strength of the beam through a linear interpolation between the calculated LTB strengths at 100 °C and 400 °C considering its actual temperature T value. The reason behind this interpolation is that the design formulae proposed in this paper have been established considering the elevated temperature LTB response of steel beams and do not provide the same room temperature LTB strengths as those determined through the LTB design equations of prEN 1993-1-1 [6]. The high accuracy of the interpolation approach

is shown in Fig. 17 for the LTB strength predictions of hot-rolled and welded steel beams with IPE 500, IPE 80 and HEM 200 sections at the elevated temperature level of 200 °C.

7. Conclusions

In this paper, the behaviour and design of laterally unrestrained steel beams susceptible to lateral-torsional buckling (LTB) in fire were investigated. Finite element models of steel beams able to replicate their LTB behaviour at elevated temperatures were developed and validated against experimental results from the literature. Using the validated finite element models, extensive parametric studies were carried out so as to explore the LTB response of steel beams in fire, taking into consideration various cross-section shapes, elevated temperature levels, steel grades and member slendernesses. It was observed that the beam cross-section shape has a rather significant influence on the LTB response of steel beams in fire and its influence should be taken into consideration through the modification of the LTB design curves in the fire design of steel beams. The results of the parametric studies also suggested that LTB design curves should be modified considering the grade of steel, while the influence of residual stresses on the LTB strengths of steel beams in fire was found low in accordance with the observations of [31, 32]. The accuracy of the existing beam buckling design rules of EN 1993-1-2 [1] was assessed, where it was observed that there is room for improvement of the accuracy of these design rules. Using a Perry-Robertson equation able to provide a sound representation of the LTB response of steel beams, a new LTB assessment equation for steel beams in fire was put forward and calibrated against the results from the extensive parametric studies carried out through the finite element models. The higher accuracy of the proposed beam buckling design method against the LTB assessment design rules of EN 1993-1-2 [1] was illustrated. The reliability of the proposed design method was also assessed against the reliability criteria put forward by Kruppa [40] for the fire design of structural steel elements, where it satisfied all the reliability criteria of Kruppa [40] unlike the beam buckling design rules of EN 1993-1-2 [1] which failed to fulfil some of the reliability criteria of [40]. It should be noted that the design equations proposed in this paper for the LTB assessment of steel beams in fire are compatible with the room temperature LTB assessment rules due to be incorporated into the upcoming version of EN 1993-1-1 [5], which is currently referred to as prEN 1993-1-1 [6]. In this study, the LTB behaviour and design of steel beams not susceptible to local buckling and subjected to constant bending moments were investigated. Future research will be directed towards the extension of the proposed design approach to steel beams undergoing interactive local and global buckling in fire taking into account the recommendations of [21, 41–46] with respect to the local instability of steel sections in fire, steel beams with non-uniform temperature distributions [47–49], high-strength steel beams [50] and steel beams subjected to varying bending moments along their lengths [12, 51].

References

- [1] EN 1993-1-2, Eurocode 3 Design of steel structures-Part 1-2: General rules – Structural fire design. European Committee for Standardization (CEN), Brussels; 2005.

- [2] Ayrton, W., Perry, J.. On struts. *The Engineer* 1886;62:464–465.
- [3] Robertson, A.. The strength of struts. *The Institution of Civil Engineers (ICE) – Selected Engineering Papers* 1925;1(28):1–55.
- [4] Taras, A., Greiner, R.. New design curves for lateral–torsional buckling—Proposal based on a consistent derivation. *Journal of Constructional Steel Research* 2010;66(5):648–663.
- [5] EN 1993-1-1, Eurocode 3 Design of steel structures-Part 1-1: General rules and rules for buildings. European Committee for Standardization (CEN), Brussels; 2005.
- [6] prEN 1993-1-1, Final Draft of Eurocode 3 Design of steel structures-Part 1-1: General rules and rules for buildings. European Committee for Standardization (CEN), Brussels; 2018.
- [7] Vila Real, P.M.M., Franssen, J.M.. Numerical modeling of lateral-torsional buckling of steel I-beams under fire conditions—Comparison with Eurocode 3. *Journal of Fire Protection Engineering* 2001;11(2):112–128.
- [8] Vila Real, P.M.M., Lopes, N., Simoes da Silva, L., Franssen, J.M.. Parametric analysis of the lateral–torsional buckling resistance of steel beams in case of fire. *Fire Safety Journal* 2007;42(6-7):416–424.
- [9] Vila Real, P.M.M., Lopes, N., Simoes da Silva, L., Franssen, J.M.. Lateral-torsional buckling of unrestrained steel beams under fire conditions: Improvement of EC3 proposal. *Computers & Structures* 2004;82(20-21):1737–1744.
- [10] Dharma, R.B., Tan, K.H.. Proposed design methods for lateral torsional buckling of unrestrained steel beams in fire. *Journal of Constructional Steel Research* 2007;63(8):1066–1076.
- [11] Couto, C., Vila Real, P.M.M., Lopes, N., Zhao, B.. Numerical investigation of the lateral–torsional buckling of beams with slender cross sections for the case of fire. *Engineering Structures* 2016;106:410–421.
- [12] Couto, C., Maia, É., Vila Real, P.M.M., Lopes, N.. The effect of non-uniform bending on the lateral stability of steel beams with slender cross-section at elevated temperatures. *Engineering Structures* 2018;163:153–166.
- [13] Abaqus 2018 Reference Manual. Simulia, Dassault Systemes; 2018.
- [14] Kucukler, M., Gardner, L., Macorini, L.. Lateral–torsional buckling assessment of steel beams through a stiffness reduction method. *Journal of Constructional Steel Research* 2015;109:87–100.
- [15] Kucukler, M., Gardner, L., Macorini, L.. Flexural–torsional buckling assessment of steel beam–columns through a stiffness reduction method. *Engineering Structures* 2015;101:662–676.
- [16] Kucukler, M., Gardner, L.. Design of laterally restrained web-tapered steel structures through a stiffness reduction method. *Journal of Constructional Steel Research* 2018;141:63–76.
- [17] He, Y., Wang, Y.. Load–deflection behaviour of thin-walled bolted plates in shear at elevated temperatures. *Thin-Walled Structures* 2016;98:127–142.
- [18] Ozyurt, E., Wang, Y., Tan, K.H.. Elevated temperature resistance of welded tubular joints under axial load in the brace member. *Engineering Structures* 2014;59:574–586.
- [19] Fung, T.C., Tan, K.H., Nguyen, M.P.. Structural behavior of chs t-joints subjected to static in-plane bending in fire conditions. *Journal of Structural Engineering, ASCE* 2015;142(3):04015155.
- [20] Laím, L., Rodrigues, J.P.C.. Numerical analysis on axially-and-rotationally restrained cold-formed steel beams subjected to fire. *Thin-Walled Structures* 2016;104:1–16.
- [21] Selamet, S., Garlock, M.E.. Predicting the maximum compressive beam axial force during fire considering local buckling. *Journal of Constructional Steel Research* 2012;71:189–201.
- [22] Rubert, A., Schaumann, P.. Structural steel and plane frame assemblies under fire action. *Fire Safety Journal* 1986;10(3):173–184.
- [23] ECCS, Ultimate limit state calculation of sway frames with rigid joints. Tech. Rep.; No. 33, Technical Committee 8 (TC 8) of European Convention for Constructional Steelwork (ECCS); 1984.
- [24] Crisfield, M.A.. A fast incremental/iterative solution procedure that handles “snap-through”. *Computers & Structures* 1981;13(1-3):55–62.
- [25] Ramm, E.. Strategies for tracing the nonlinear response near limit points. In: *Nonlinear finite element analysis in structural mechanics*. Springer; 1981, p. 63–89.
- [26] Mesquita, L., Piloto, P., Vaz, M., Vila Real, P.M.M.. Experimental and numerical research on the

- critical temperature of laterally unrestrained steel I beams. *Journal of Constructional Steel Research* 2005;61(10):1435–1446.
- [27] Rebelo, C., Lopes, N., Simoes da Silva, L., Nethercot, D., Vila Real, P.M.M.. Statistical evaluation of the lateral-torsional buckling resistance of steel I-beams, Part 1: Variability of the Eurocode 3 resistance model. *Journal of Constructional Steel Research* 2009;65(4):818–831.
- [28] Boissonnade, N., Somja, H.. Influence of imperfections in FEM modeling of lateral torsional buckling. In: *Proceeding of the Annual Stability Conference Structural Stability Research Council*. 2012, p. 18–21.
- [29] Subramanian, L., White, D.W.. Resolving the disconnects between lateral torsional buckling experimental tests, test simulations and design strength equations. *Journal of Constructional Steel Research* 2017;128:321–334.
- [30] Trahair, N.S.. Inelastic lateral buckling of continuous steel beams. *Engineering Structures* 2019;190:238–245.
- [31] Franssen, J.M.. Residual stresses in steel profiles submitted to the fire: An analogy. In: *Proc. 3rd CIB/W14 FSF workshop on modelling*. TNO Building and Construction Research; 1996, p. 103–112.
- [32] Vila Real, P.M.M., Cazeli, R., Simoes da Silva, L., Santiago, A., Piloto, P.. The effect of residual stresses in the lateral-torsional buckling of steel I-beams at elevated temperature. *Journal of Constructional Steel Research* 2004;60(3-5):783–793.
- [33] Talamona, D., Franssen, J.M., Schleich, J.B., Kruppa, J.. Stability of steel columns in case of fire: Numerical modeling. *Journal of Structural Engineering, ASCE* 1997;123(6):713–720.
- [34] Franssen, J.M., Talamona, D., Kruppa, J., Cajot, L.G.. Stability of steel columns in case of fire: Experimental evaluation. *Journal of Structural Engineering, ASCE* 1998;124(2):158–163.
- [35] Kucukler, M., Gardner, L.. Design of web-tapered steel beams against lateral-torsional buckling through a stiffness reduction method. *Engineering Structures* 2019;190:246–261.
- [36] Maquoi, R., Rondal, J.. Mise en equation des nouvelles courbes Européennes de flambement. *Construction Métallique* 1978;1:17–30.
- [37] Rondal, J., Maquoi, R.. Formulations d'ayrton-perry pour le flambement des barres métalliques. *Construction Métallique* 1979;4:41–53.
- [38] EN 1090-2, Execution of Steel Structures and Aluminium Structures-Part 2: Technical Requirements for Steel Structures. European Committee for Standardization (CEN), Brussels; 2018.
- [39] Kucukler, M., Xing, Z., Gardner, L.. Behaviour and design of stainless steel I-section columns in fire. *Journal of Constructional Steel Research* 2020;165:105890.
- [40] Kruppa, J.. Eurocodes–Fire parts: Proposal for a methodology to check the accuracy of assessment methods. CEN TC 250, Horizontal Group Fire, Document no: 99/130; 1999.
- [41] Knobloch, M., Fontana, M.. Strain-based approach to local buckling of steel sections subjected to fire. *Journal of Constructional Steel Research* 2006;62(1-2):44–67.
- [42] Heidarpour, A., Bradford, M.A.. Local buckling and slenderness limits for steel webs under combined bending, compression and shear at elevated temperatures. *Thin-Walled Structures* 2008;46(2):128–146.
- [43] Quiel, S.E., Garlock, M.E.. Calculating the buckling strength of steel plates exposed to fire. *Thin-Walled Structures* 2010;48(9):684–695.
- [44] Knobloch, M., Pauli, J., Somaini, D., Fontana, M.. Stress-strain response and cross-sectional capacity of steel sections in fire. *Proceedings of the Institution of Civil Engineers-Structures and Buildings* 2013;166(8):444–455.
- [45] Couto, C., Real, P.V., Lopes, N., Zhao, B.. Resistance of steel cross-sections with local buckling at elevated temperatures. *Journal of Constructional Steel Research* 2015;109:101–114.
- [46] Xing, Z., Kucukler, M., Gardner, L.. Local buckling of stainless steel plates in fire. *Thin-Walled Structures* 2020;148:106570.
- [47] Yin, Y.Z., Wang, Y.C.. Analysis of catenary action in steel beams using a simplified hand calculation method, Part 2: Validation for non-uniform temperature distribution. *Journal of Constructional Steel Research* 2005;61(2):213–234.
- [48] Zhang, C., Li, G.Q., Usmani, A.. Simulating the behavior of restrained steel beams to flame

- impingement from localized-fires. *Journal of Constructional Steel Research* 2013;83:156–165.
- [49] Zhang, C., Gross, J.L., McAllister, T.P.. Lateral-torsional buckling of steel W-beams subjected to localized fires. *Journal of Constructional Steel Research* 2013;88:330–338.
- [50] Varol, H., Cashell, K.. Numerical modelling of high strength steel beams at elevated temperature. *Fire Safety Journal* 2017;89:41–50.
- [51] Bailey, C., Burgess, I., Plank, R.. The lateral-torsional buckling of unrestrained steel beams in fire. *Journal of Constructional Steel Research* 1996;36(2):101–119.

Figures captions

Figure 1 : Stress-strain relationship and material property reduction factors for carbon steel at elevated temperatures adopted in this study as given in [1]

Figure 2 : Stress-strain response of grade S355 carbon steel at different elevated temperature levels

Figure 3 : Definition of the geometric imperfections in the finite element models using the global buckling modes

Figure 4 : Residual stress patterns applied to the finite element models (+ve tension, -ve compression)

Figure 5 : Comparison of the temperature versus mid-span vertical displacement paths obtained from the finite element models herein against those obtained from physical experiments by Mesquita et al. [26]

Figure 6 : Change of $\sqrt{k_{y,\theta,com}/k_{E,\theta,com}}$ for different elevated temperature levels

Figure 7 : Influence of cross-section shape on the LTB response of steel beams in fire for different elevated temperature levels

Figure 8 : Influence of the grade of steel on the LTB response of steel beams in fire for different elevated temperature levels

Figure 9 : Influence residual stresses on the LTB response of steel beams in fire for different elevated temperature levels

Figure 10 : Reduction of residual stresses within the finite element models of steel beams with increasing elevated temperature levels (stresses in MPa)

Figure 11 : Influence of the elevated temperature level on the LTB strengths of steel beams normalised by the elevated temperature plastic bending moment resistances $M_{y,Ed}/(W_{pl,y}k_{y,\theta}f_y)$

Figure 12 : Fork-end supported I-section steel beam under constant major axis bending M_y in fire and the internal moments arising within the mid-span section

Figure 13 : Calibration of the generalised imperfection factor η_{LT} using the GMNIA results of fork-end supported beams subjected to uniform major axis bending at different elevated temperature levels

Figure 14 : Accuracy of the proposed beam buckling design rules for beams with different cross-sections undergoing LTB at different elevated temperature levels

Figure 15 : Accuracy of the new proposals against the beam buckling design rules of EN 1993-1-2 [1] for hot-rolled steel beams in fire

Figure 16 : Accuracy of the new proposals against the beam buckling design rules of EN 1993-1-2 [1] for welded steel beams in fire

Figure 17 : Accuracy of the proposed design method when applied in conjunction with the described interpolation approach for hot-rolled and welded steel beams at the elevated temperature level of 200 °C

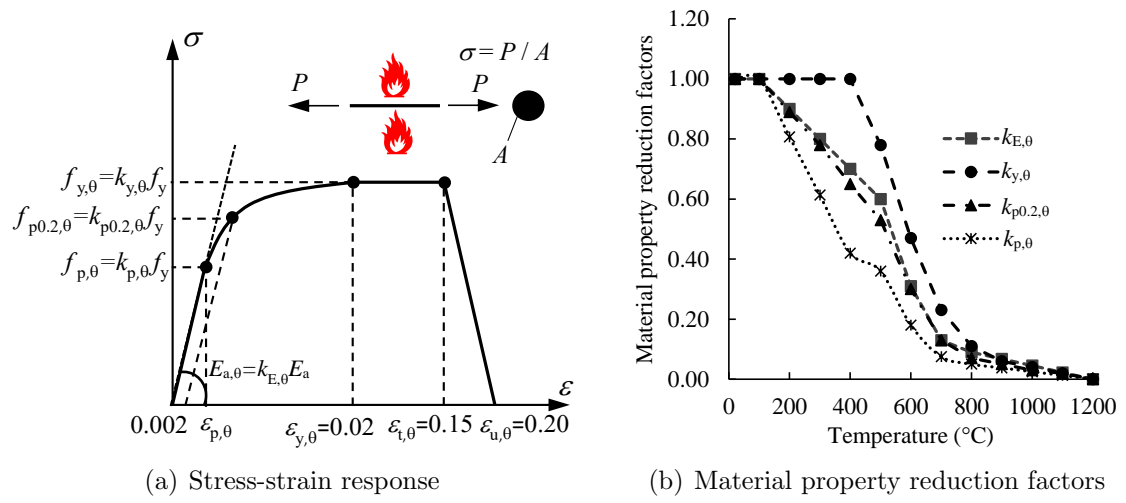


Figure 1: Stress-strain relationship and material property reduction factors for carbon steel at elevated temperatures adopted in this study as given in [1]

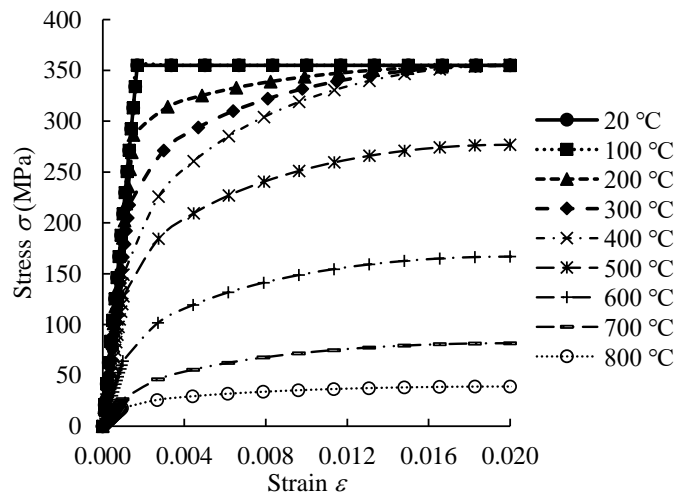


Figure 2: Stress-strain response of grade S355 carbon steel at different elevated temperature levels

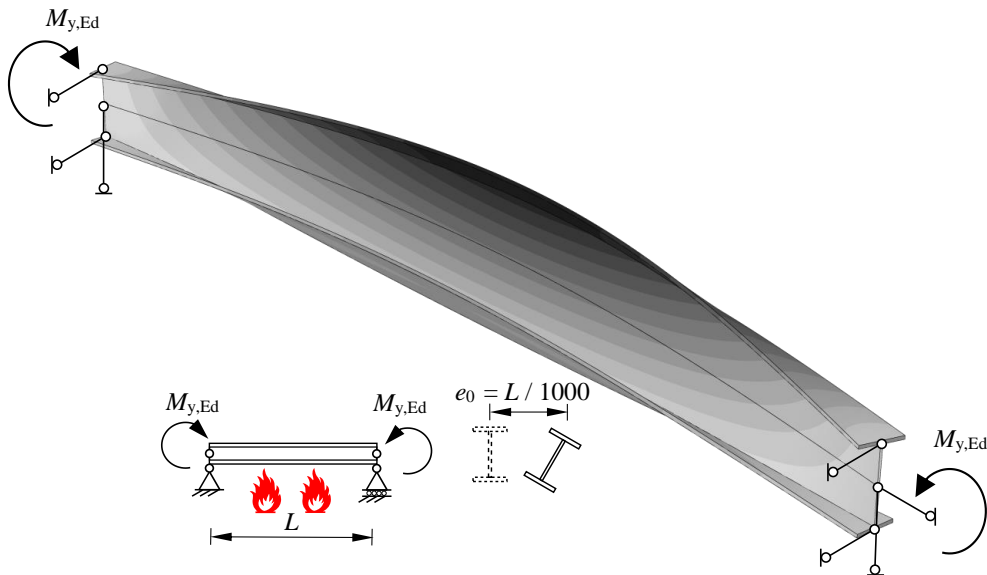


Figure 3: Definition of the geometric imperfections in the finite element models using the global buckling modes

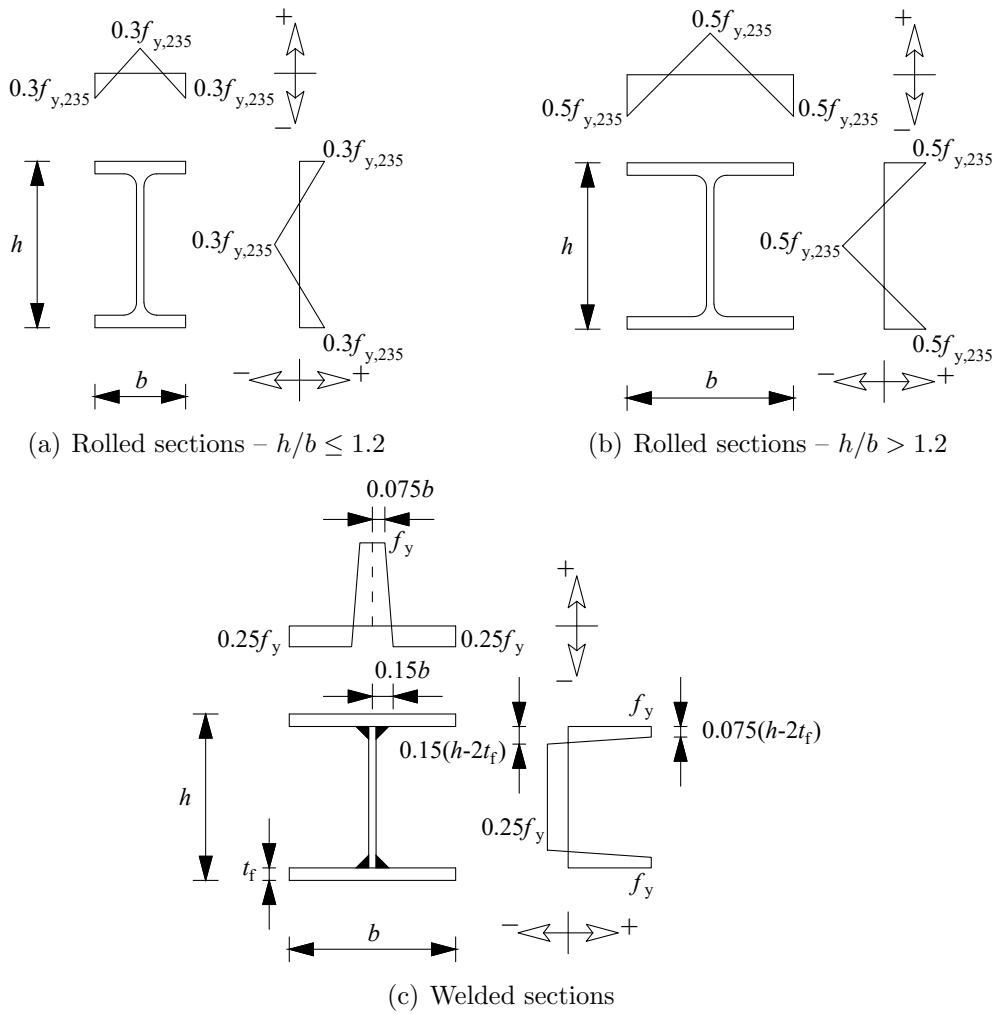


Figure 4: Residual stress patterns applied to the finite element models (+ve tension, -ve compression)

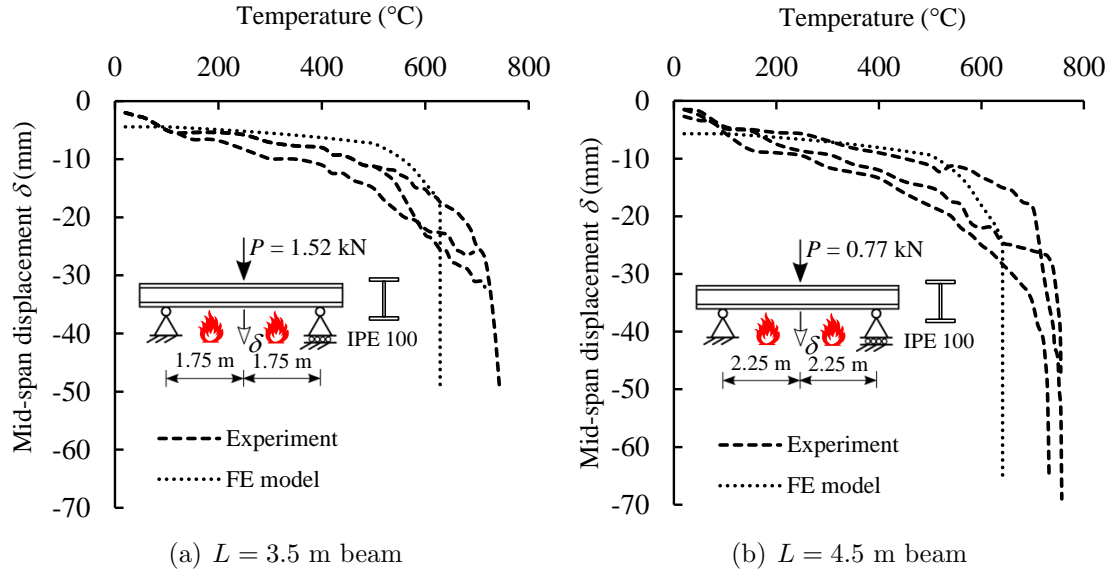


Figure 5: Comparison of the temperature versus mid-span vertical displacement paths obtained from the finite element models herein against those obtained from physical experiments by Mesquita et al. [26]

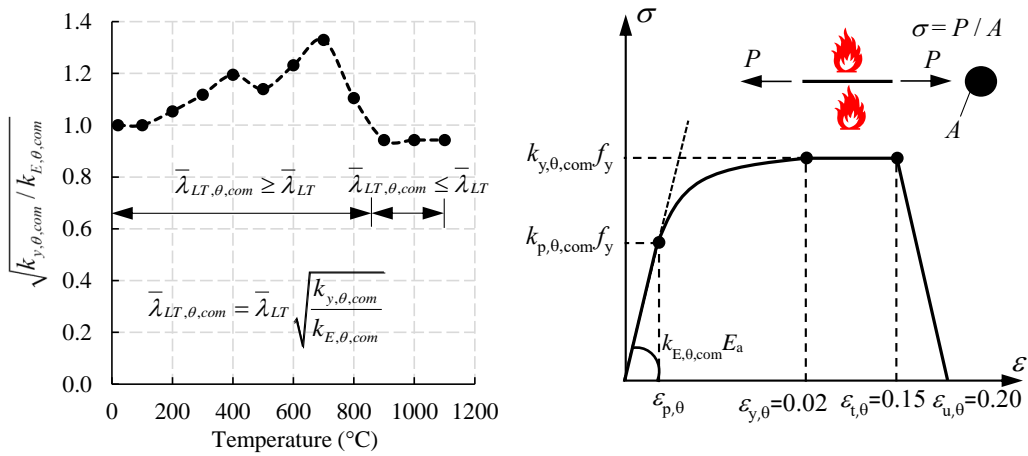


Figure 6: Change of $\sqrt{k_{y,\theta,com}/k_{E,\theta,com}}$ for different elevated temperature levels

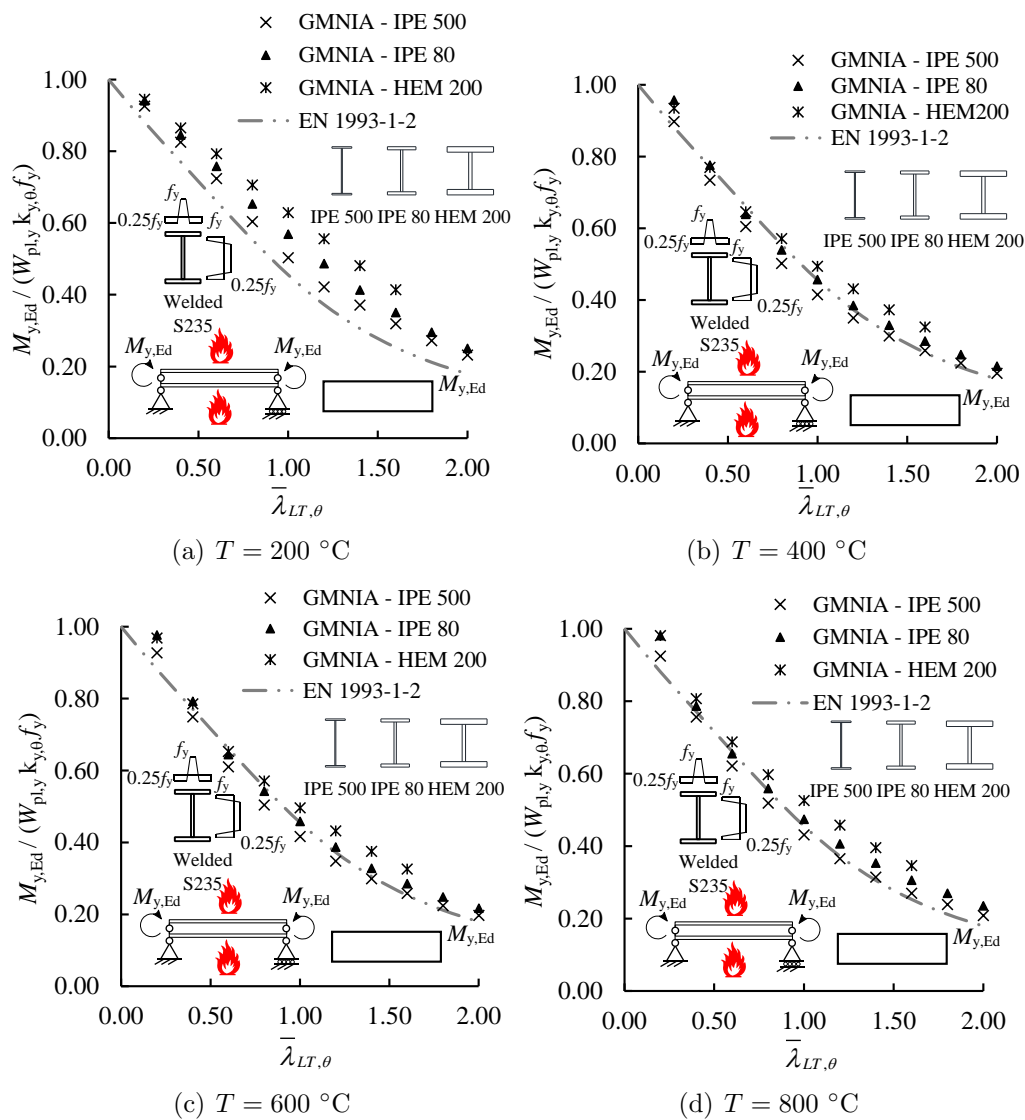


Figure 7: Influence of cross-section shape on the LTB response of steel beams in fire for different elevated temperature levels

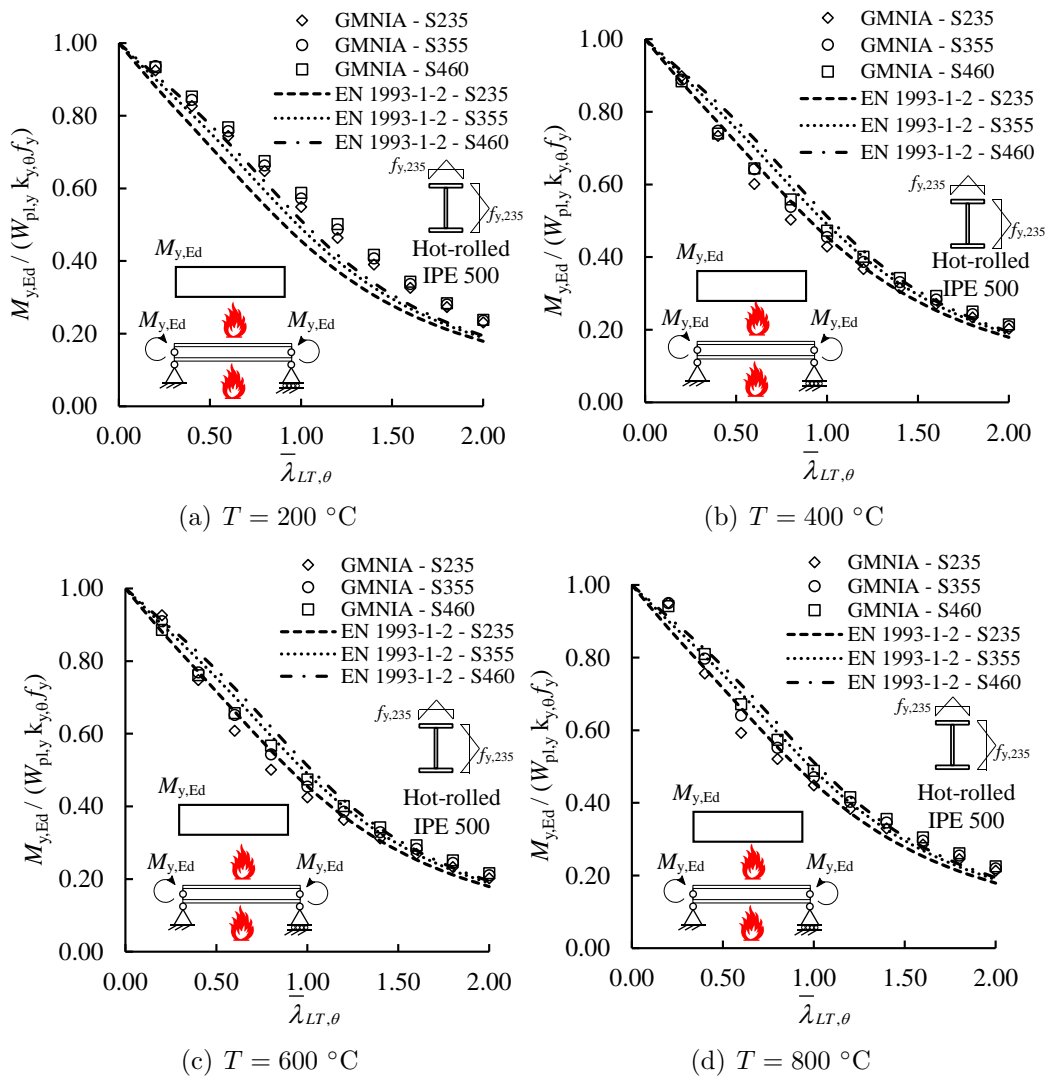


Figure 8: Influence of the grade of steel on the LTB response of steel beams in fire for different elevated temperature levels

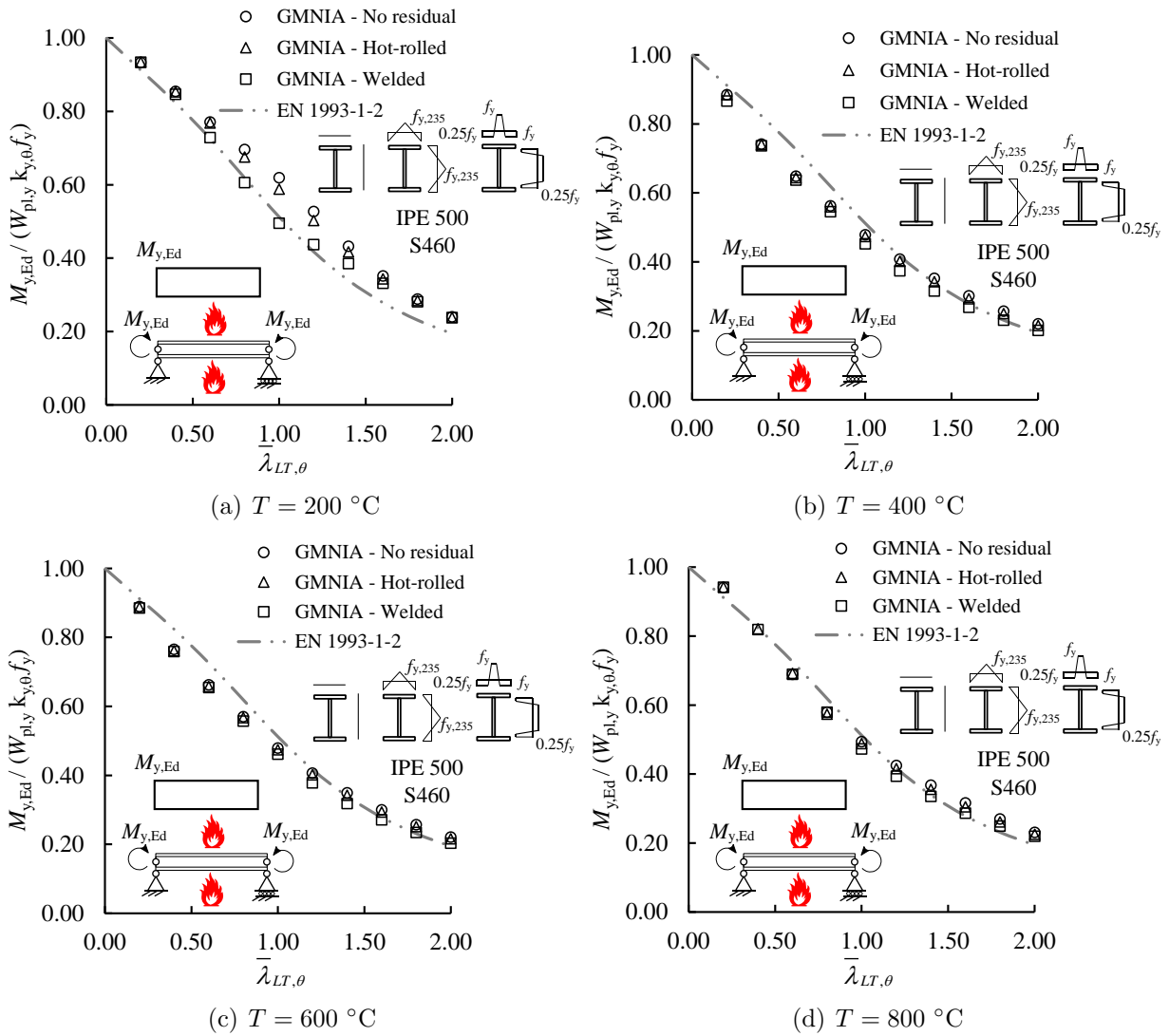


Figure 9: Influence residual stresses on the LTB response of steel beams in fire for different elevated temperature levels

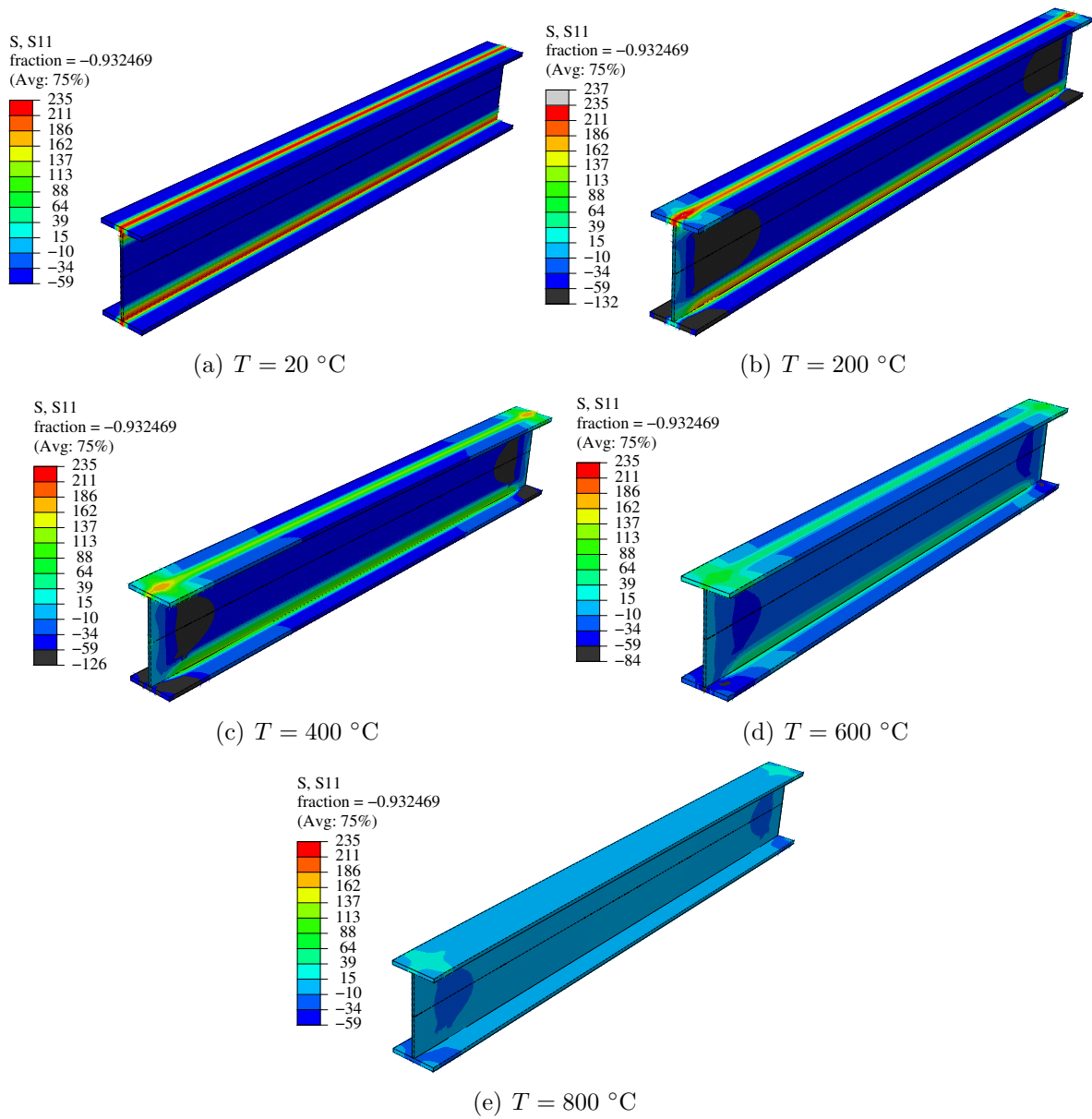


Figure 10: Reduction of residual stresses within the finite element models of steel beams with increasing elevated temperature levels (stresses in MPa)

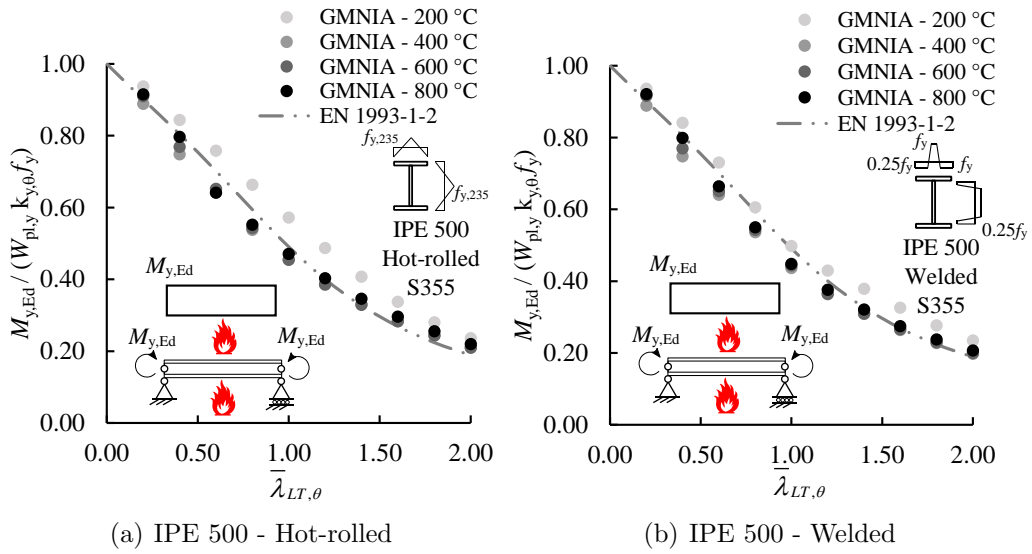


Figure 11: Influence of the elevated temperature level on the LTB strengths of steel beams normalised by the elevated temperature plastic bending moment resistances $M_{y,Ed}/(W_{pl,y}k_{y,\theta}f_y)$

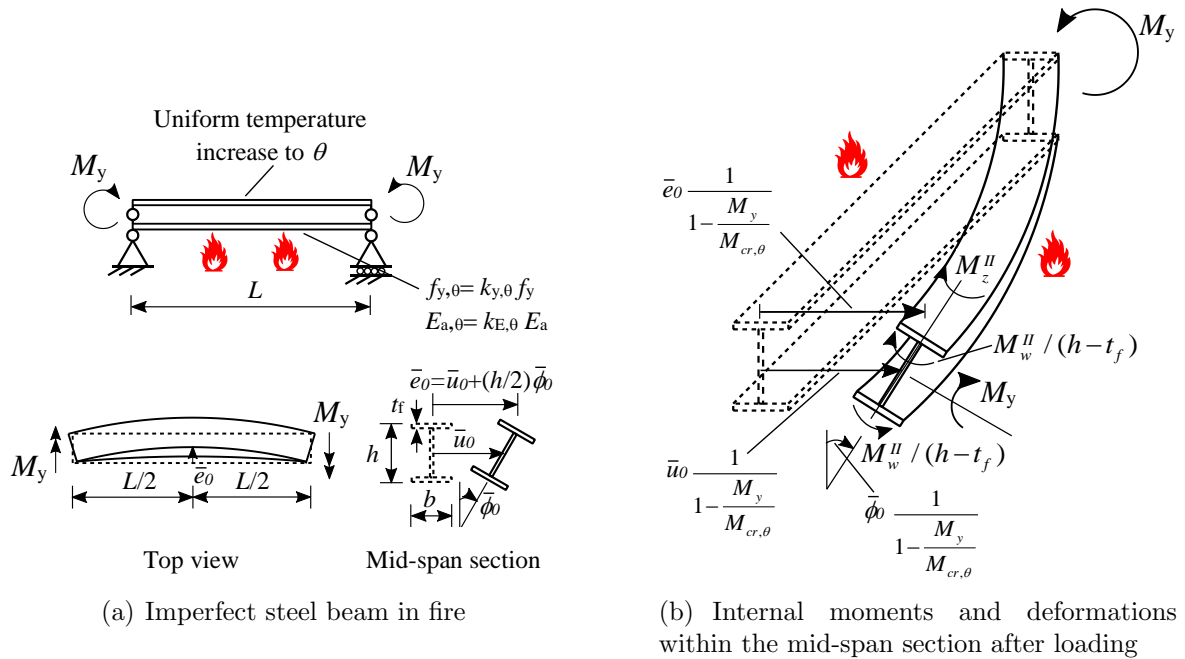
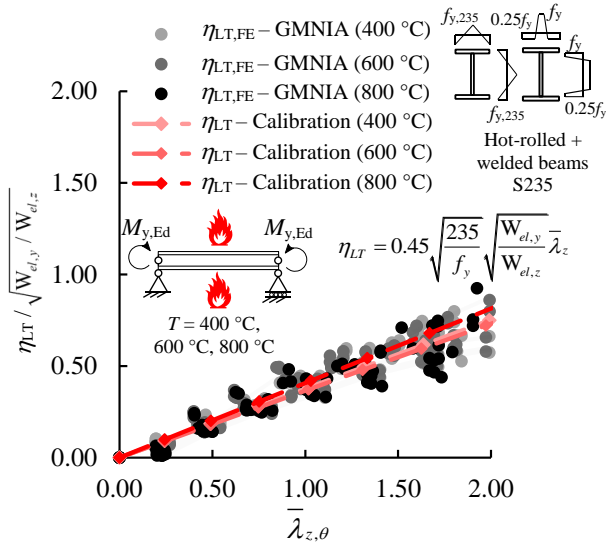
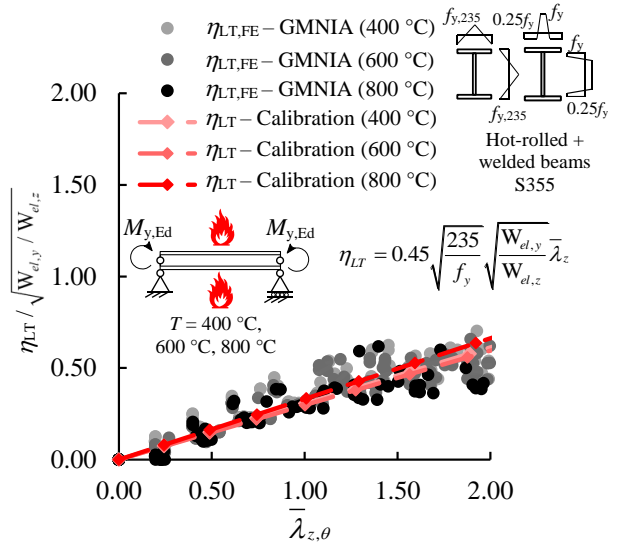


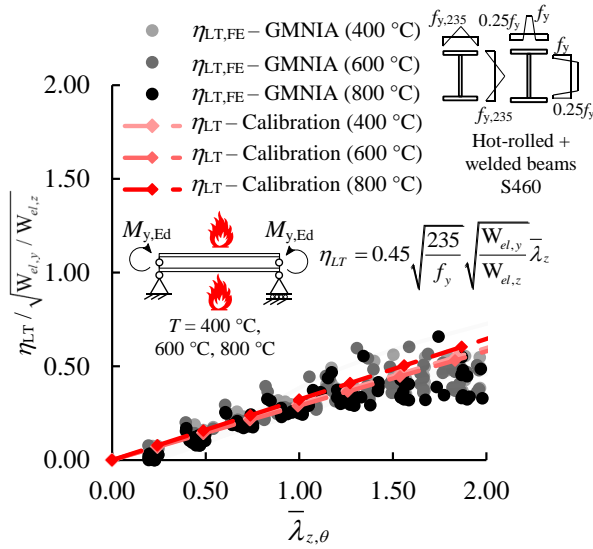
Figure 12: Fork-end supported I-section steel beam under constant major axis bending M_y in fire and the internal moments arising within the mid-span section



(a) Grade S235 steel beams



(b) Grade S355 steel beams



(c) Grade S460 steel beams

Figure 13: Calibration of the generalised imperfection factor η_{LT} using the GMNIA results of fork-end supported beams subjected to uniform major axis bending at different elevated temperature levels

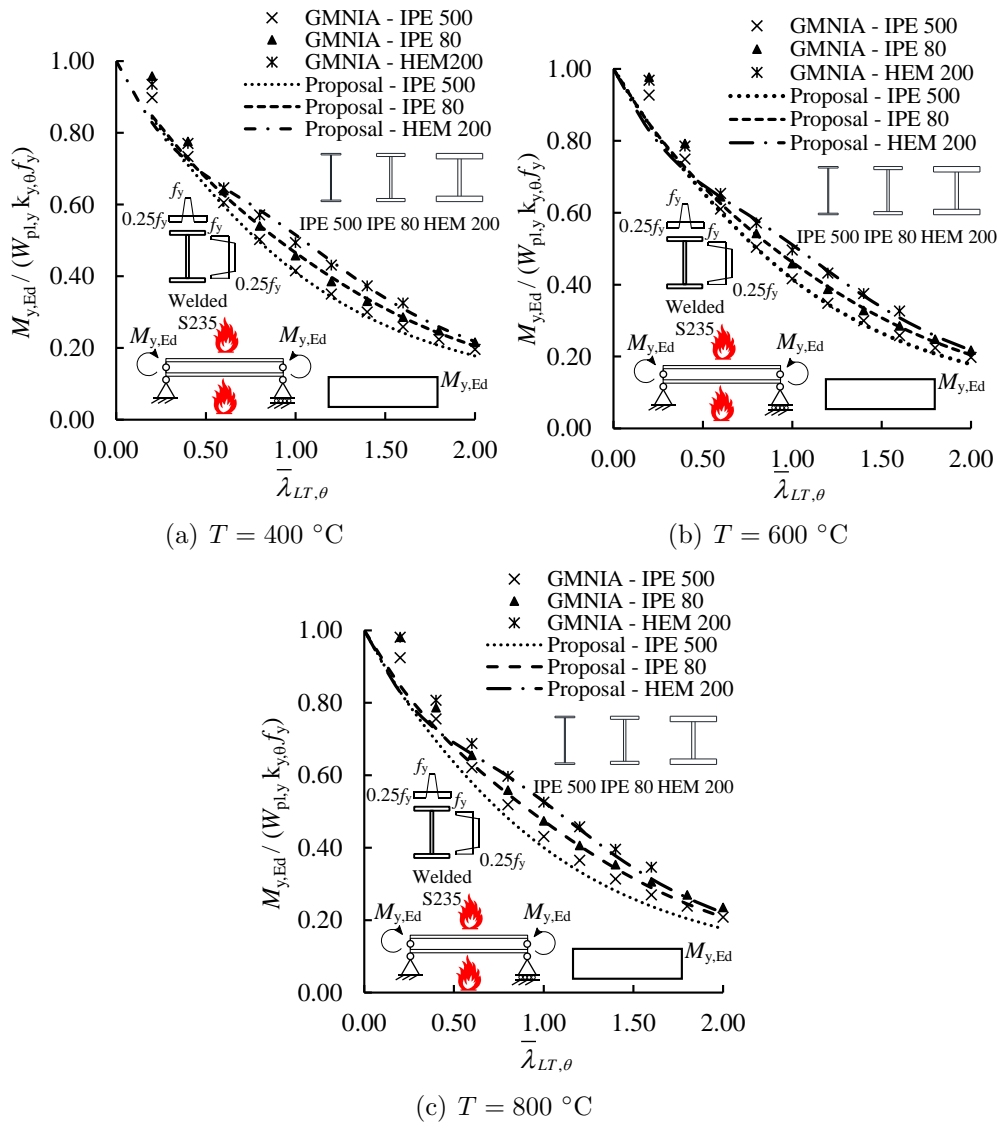


Figure 14: Accuracy of the proposed beam buckling design rules for beams with different cross-sections undergoing LTB at different elevated temperature levels

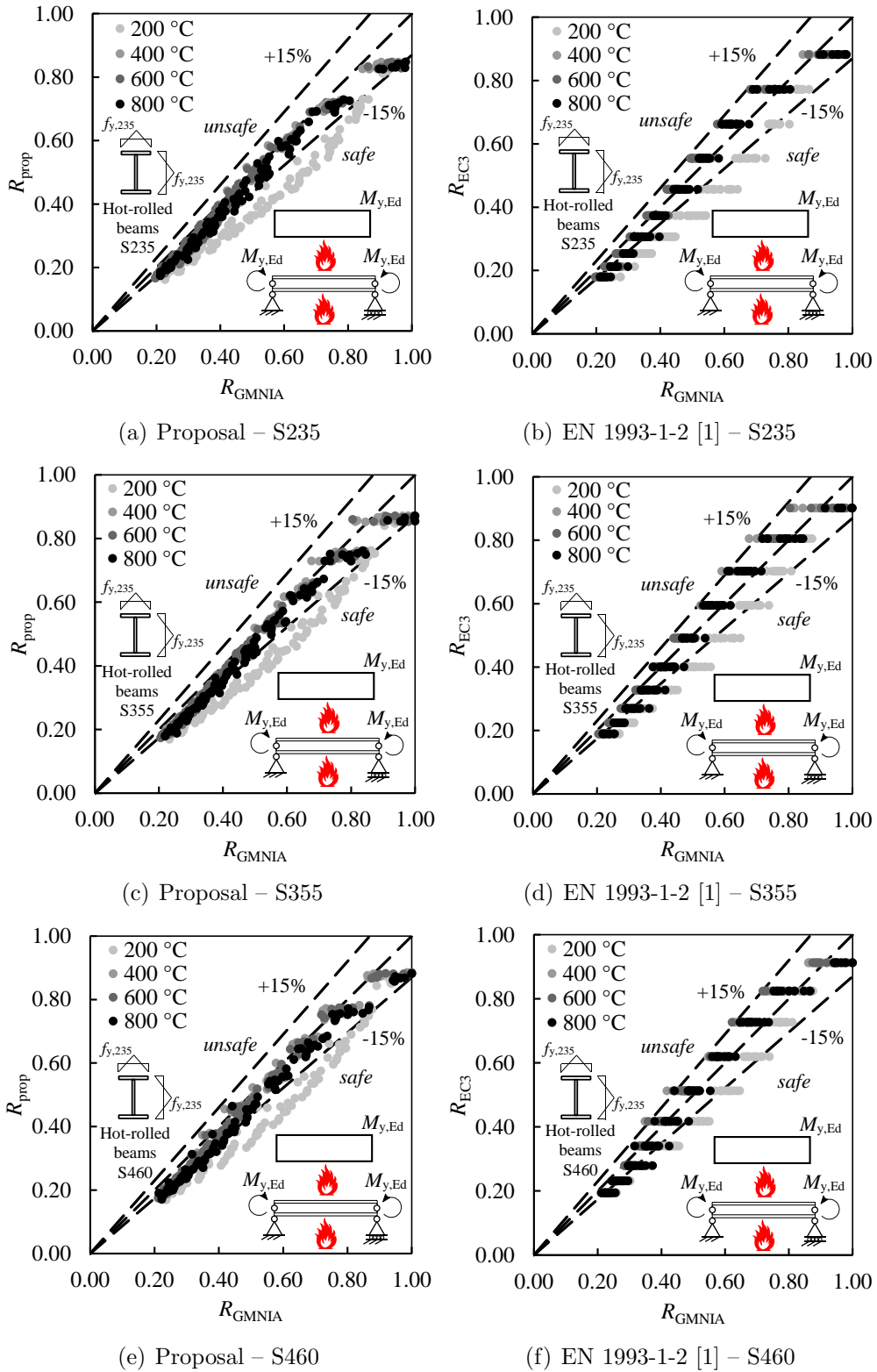


Figure 15: Accuracy of the new proposals against the beam buckling design rules of EN 1993-1-2 [1] for hot-rolled steel beams in fire

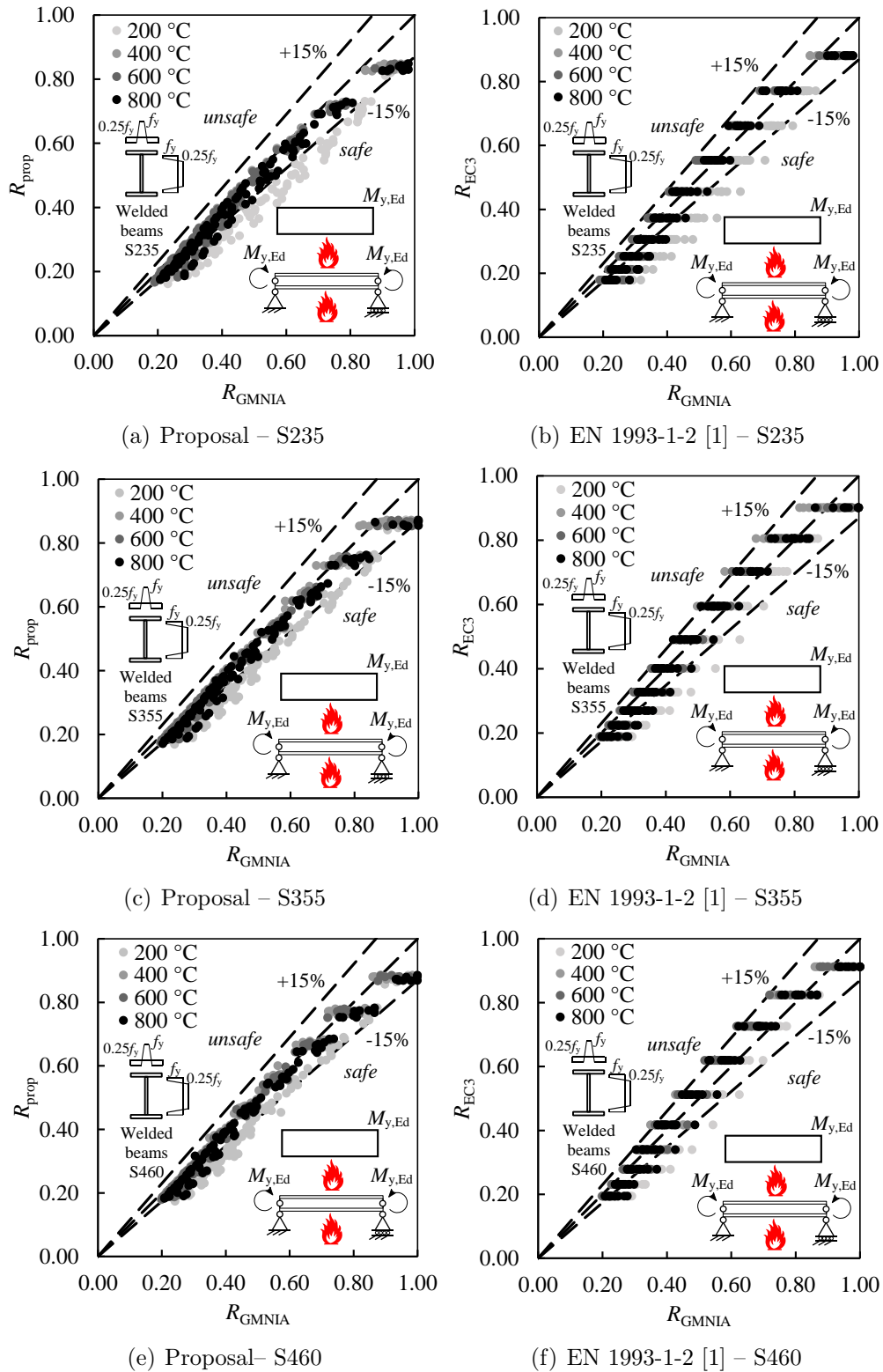


Figure 16: Accuracy of the new proposals against the beam buckling design rules of EN 1993-1-2 [1] for welded steel beams in fire

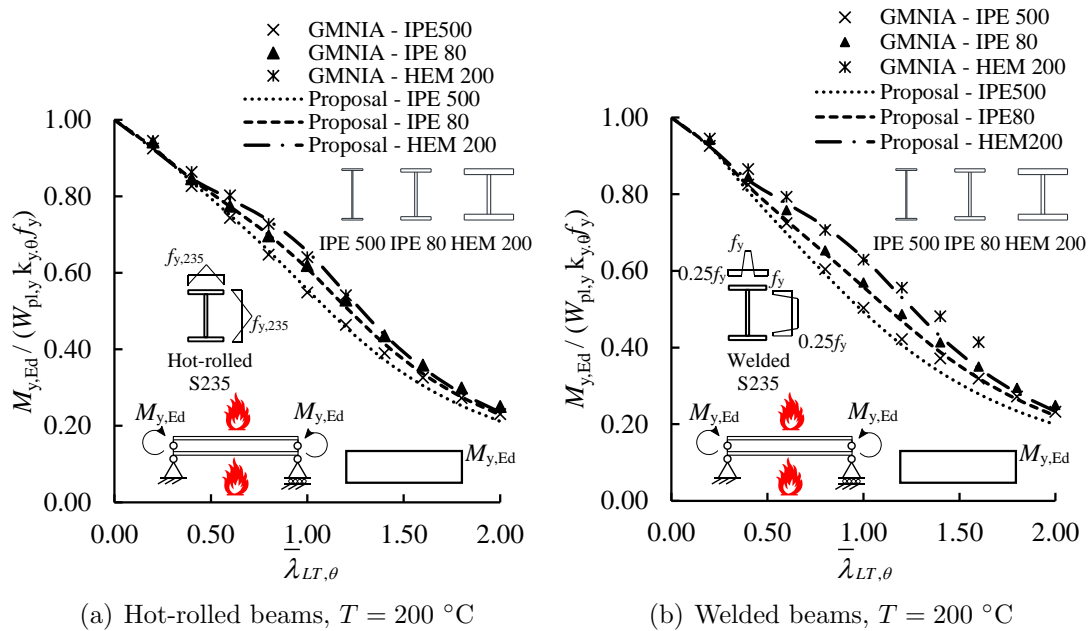


Figure 17: Accuracy of the proposed design method when applied in conjunction with the described interpolation approach for hot-rolled and welded steel beams at the elevated temperature level of $200 \text{ }^\circ\text{C}$

Tables captions

Table 1 : Comparison of the critical temperatures obtained from the finite element models $\theta_{cr,FE}$ ($^{\circ}\text{C}$) against those obtained from experiments $\theta_{cr,test}$ by Mesquita et al. [26]

Table 2 : Summary of the parametric studies carried out in this paper

Table 3 : Accuracy of the proposed design method and EN 1993-1-2 for the lateral-torsional buckling (LTB) assessment of steel beams in fire

Table 4 : Reliability of the proposed design method and EN 1993-1-2 for the lateral-torsional buckling (LTB) assessment of steel beams in fire on the basis of the reliability criteria set out by Kruppa. Note that the numbers denoted by * violates the corresponding criterion

Table 1: Comparison of the critical temperatures obtained from the finite element models $\theta_{cr,FE}$ ($^{\circ}\text{C}$) against those obtained from experiments $\theta_{cr,test}$ by Mesquita et al. [26]

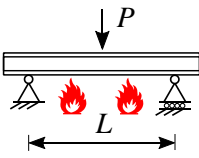
Loading conditions	Specimen	L (m)	P (kN)	$\theta_{cr,test}$ ($^{\circ}\text{C}$)	$\theta_{cr,FE}$ ($^{\circ}\text{C}$)	$\theta_{cr,FE}/\theta_{cr,test}$
	L1.5-1			717		0.90
	L1.5-2	1.5	6.09	690	647	0.94
	L1.5-3			705		0.92
	L2-1			770		0.81
	L2-2	2.0	4.32	606	622	1.03
	L2-3			665		0.94
	L2.5-1			732		0.84
	L2.5-2	2.5	3.04	740	614	0.83
	L2.5-3			740		0.83
	L3.5-1			744		0.83
	L3.5-2	3.5	1.52	693	621	0.90
	L3.5-3			715		0.87
	L4.5-1			732		0.87
	L4.5-2	4.5	0.77	757	634	0.84
	L4.5-3			756		0.84
					$\left(\frac{\theta_{cr,FE}}{\theta_{cr,test}}\right)_{av}$	0.88
					$\left(\frac{\theta_{cr,FE}}{\theta_{cr,test}}\right)_{COV}$	0.081

Table 2: Summary of the parametric studies carried out in this paper

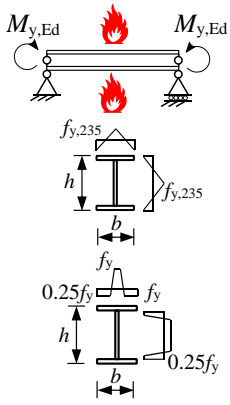
Loading condition	Cross-section (h/b)	Steel grades	Fabrication process	Temperature	Slenderness $\bar{\lambda}_{LT,\theta}$
	IPE 500 (2.50)				0.2
	IPE 240 (2.00)				0.4
	IPE 80 (1.74)				0.6
	IPE 600 (2.72)				0.8
	HEM 200 (1.07)	S235	Hot-rolled	200 $^{\circ}\text{C}$	1.0
	HEB 400 (1.33)	S355	Welded	400 $^{\circ}\text{C}$	1.2
	HEAA 1000 (3.23)	S460		600 $^{\circ}\text{C}$	1.4
	HEM 600 (2.03)			800 $^{\circ}\text{C}$	1.6
	HEB 600 (2.00)				1.8
	HEA 200 (0.95)				2.0
	HEAA 200 (0.93)				
	HEAA 450 (1.42)				

Table 3: Accuracy of the proposed design method and EN 1993-1-2 for the lateral-torsional buckling (LTB) assessment of steel beams in fire

	Steel grade	N	ϵ_{av}	ϵ_{COV}	ϵ_{max}	ϵ_{min}
Proposed design method	S235	672	1.09	0.072	1.52	0.94
	S355	683	1.08	0.071	1.47	0.93
	S460	672	1.07	0.072	1.42	0.92
EN 1993-1-2 [1]	S235	672	1.05	0.111	1.58	0.87
	S355	683	1.03	0.107	1.50	0.83
	S460	672	1.01	0.103	1.43	0.82
Vila Real et al. [8]	S235	672	1.08	0.108	1.61	0.89
	S355	683	1.05	0.101	1.53	0.87
	S460	672	1.05	0.099	1.47	0.87

Table 4: Reliability of the proposed design method and EN 1993-1-2 for the lateral-torsional buckling (LTB) assessment of steel beams in fire on the basis of the reliability criteria set out by Kruppa. Note that the numbers denoted by * violates the corresponding criterion

	Steel grade	Criterion 1	Criterion 2	Criterion 3
Proposed design method	S235	0.00	5.45	-11.08
	S355	0.00	6.70	-9.84
	S460	0.00	15.09	-8.63
EN 1993-1-2 [1]	S235	0.00	30.03*	-7.48
	S355	1.32*	37.87*	-4.70
	S460	2.29*	43.20*	-3.07
Vila Real et al. [8]	S235	0.00	21.02*	-9.94
	S355	0.00	29.53*	-6.93
	S460	0.00	28.69*	-6.88